



Multimodal Imaging Mass Spectrometry: Next Generation Molecular Mapping in Biology and Medicine

Elizabeth Kathleen Neumann, Katerina Djambazova, Richard M. Caprioli, and Jeffrey M. Spraggins

J. Am. Soc. Mass Spectrom., Just Accepted Manuscript • DOI: 10.1021/jasms.0c00232 • Publication Date (Web): 31 Jul 2020

Downloaded from pubs.acs.org on August 15, 2020

Just Accepted

“Just Accepted” manuscripts have been peer-reviewed and accepted for publication. They are posted online prior to technical editing, formatting for publication and author proofing. The American Chemical Society provides “Just Accepted” as a service to the research community to expedite the dissemination of scientific material as soon as possible after acceptance. “Just Accepted” manuscripts appear in full in PDF format accompanied by an HTML abstract. “Just Accepted” manuscripts have been fully peer reviewed, but should not be considered the official version of record. They are citable by the Digital Object Identifier (DOI®). “Just Accepted” is an optional service offered to authors. Therefore, the “Just Accepted” Web site may not include all articles that will be published in the journal. After a manuscript is technically edited and formatted, it will be removed from the “Just Accepted” Web site and published as an ASAP article. Note that technical editing may introduce minor changes to the manuscript text and/or graphics which could affect content, and all legal disclaimers and ethical guidelines that apply to the journal pertain. ACS cannot be held responsible for errors or consequences arising from the use of information contained in these “Just Accepted” manuscripts.

1
2
3
4
5
6
7
8
9

Multimodal Imaging Mass Spectrometry: Next Generation Molecular Mapping in Biology and Medicine

Elizabeth K. Neumann^{1,2}, Katerina V. Djambazova,^{2,3} Richard M. Caprioli,¹⁻⁵ and Jeffrey M. Spraggins^{1-3*}

¹Department of Biochemistry, Vanderbilt University, 607 Light Hall, Nashville, TN 37205, USA

²Mass Spectrometry Research Center, Vanderbilt University, 465 21st Ave S #9160, Nashville, TN 37235, USA

³Department of Chemistry, Vanderbilt University, 7330 Stevenson Center, Station B 351822, Nashville, TN 37235, USA

⁴Department of Pharmacology, Vanderbilt University, 2220 Pierce Avenue, Nashville, TN 37232, USA

⁵Department of Medicine, Vanderbilt University, 465 21st Ave S #9160, Nashville, TN 37235, USA

KEYWORDS. *Imaging Mass Spectrometry, Chemical Imaging, Multimodal Analysis, Tissue Analysis*

ABSTRACT: Imaging mass spectrometry has become a mature molecular mapping technology that is used for molecular discovery in many medical and biological systems. While powerful by itself, imaging mass spectrometry can be complemented by the addition of other orthogonal, chemically informative imaging technologies to maximize the information gained from a single experiment and enable deeper understanding of biological processes. Within this review, we describe MALDI, SIMS, and DESI imaging mass spectrometric technologies and how these have been integrated with other analytical modalities such as microscopy, transcriptomics, spectroscopy, and electrochemistry in a field termed multimodal imaging. We explore the future of this field and discuss forthcoming developments that will bring new insights to help unravel the molecular complexities of biological systems, from single cells to functional tissue structures and organs.

I. Introduction

Imaging mass spectrometry (IMS) is a technology that enables the mapping of hundreds to thousands of molecules within biological systems.¹⁻⁶ The instruments within the field can measure a diverse array of sample types and chemical classes, ranging from low molecular weight metabolites⁷⁻¹⁰ and signaling molecules¹¹⁻¹³ to lipids,¹⁴⁻²¹ peptides,²²⁻²⁴ and proteins.²⁵⁻²⁹ A typical IMS experiment involves defining an area of the sample surface to be imaged followed by the desorption and ionization at multiple discrete locations. Each desorbed location, or pixel, is composed of an individual mass spectrum. A molecular image is generated for each signal recorded by plotting the ion intensity of that signal throughout the array of pixels generated from the sample. While there are many types of IMS technologies that have been reported in literature, we highlight here the three most common: matrix-assisted laser desorption/ionization (MALDI),^{30,31} secondary ion mass spectrometry (SIMS),³²⁻³⁴ and desorption electrospray ionization (DESI).³⁵⁻³⁸ Additional information on other types of IMS technologies can be found in several recent reviews.^{1,4,39}

Each IMS technology can be coupled to a variety of analytical approaches to enhance the information gained in a single experiment. Although IMS provides rich, chemically informative spectra and mapping capabilities, combining this unique mass specific technology with other analytical approaches can provide additional information for an analyzed sample. Combining two or more imaging modalities is termed multimodal imaging. The accrued advantages include enhanced discrimination between modality specific chemical and instrumental noise from biologically relevant chemical signals,

improved sensitivity and specificity of chemical classes not easily analyzed by a single modality alone, and enhanced data mining capabilities. Combining IMS technologies with other analytical approaches provides a more effective means to probe the molecular complexity of biological systems. In this review, we summarize major advancements in the field of multimodal imaging mass spectrometry over the past few years and discuss the exciting future of this field.

II. Overview of Imaging Mass Spectrometry Technologies

a. Matrix-Assisted Laser Desorption/Ionization

MALDI is a common ionization method within the IMS field as it can visualize numerous molecular species over a broad mass range with great molecular diversity. For tissue analysis, sample preparation typically involves sectioning of tissues and thaw mounting these sections onto a glass slide or other target (e.g. conductive surface for high voltage ion sources) and subsequent application of an organic chemical matrix that aids in analyte desorption and ionization.⁴⁰ Spatial resolution is defined by the ablation area of the laser and the distance between pixels (pitch). A variety of matrices are used for specific molecular classes. Commonly used matrices include 2,5-dihydroxybenzoic acid⁴¹ or cyano-4-hydroxycinnamic acid⁴² for positive ion mode analysis of metabolites, lipids, and peptides. Additionally, 9-aminoacridine⁴³ is typically used for negative ion mode analysis of metabolites, lipids, and proteins, while 1,5-diaminonaphthalene⁴⁴ is employed for analysis of lipids in both ion polarities. Recently norharmane has been shown to be effective for the analysis of hydrophobic molecules and low

molecular weight metabolites.⁴⁵ Matrix deposition is often performed robotically to best balance reproducibility, analyte extraction, achieve small crystal size, and produce coating homogeneity, although sublimation, sieving, and airbrushing is also used in the field.^{4,46}

As high spatial resolution MALDI IMS capabilities are developed that approach cellular and subcellular resolutions, challenges in sensitivity arise as the number of molecules sampled decreases with smaller pixel sizes. Ultimately, spatial resolution is dependent upon multiple factors such as matrix crystal size, laser focus, and stage motor step precision. Most modern MALDI IMS platforms utilize either a frequency tripled Nd:YAG (355 nm) or nitrogen gas laser (337.7 nm) and can achieve spatial resolutions of 5-20 μm using traditional front-side laser optics.⁵²⁻⁵⁴ Improving laser focus beyond 5 μm can be achieved with more advanced setups using lower laser wavelengths (e.g. 213 nm) or changing laser geometries (e.g. transmission-mode), to minimize the effective

spot size as described in the next several examples. For instance, Heiles et al. demonstrated a new source that integrates a 213 nm laser allowing for a ~3 μm footprint using front-side laser optics.⁵⁵ Alternatively, Zavalin and coworkers developed a transmission-mode geometry MALDI source, where the UV-laser is redirected to ablate the sample from the backside. By decoupling the laser and ion optics, higher numerical aperture objectives can be utilized without impeding the ion path, resulting in ~1 μm spot sizes.⁵⁶ However, a drawback of any high spatial resolution IMS experiment is a reduction in ion abundances; the Caprioli⁵⁷ and Dreisewerd⁴⁷ labs incorporated a secondary laser perpendicular to the primary ablation plume as a means to enhance ionization of transmission geometry setups. An example of these datasets is featured here (Figure 1A).

b. Secondary Ion Mass Spectrometry

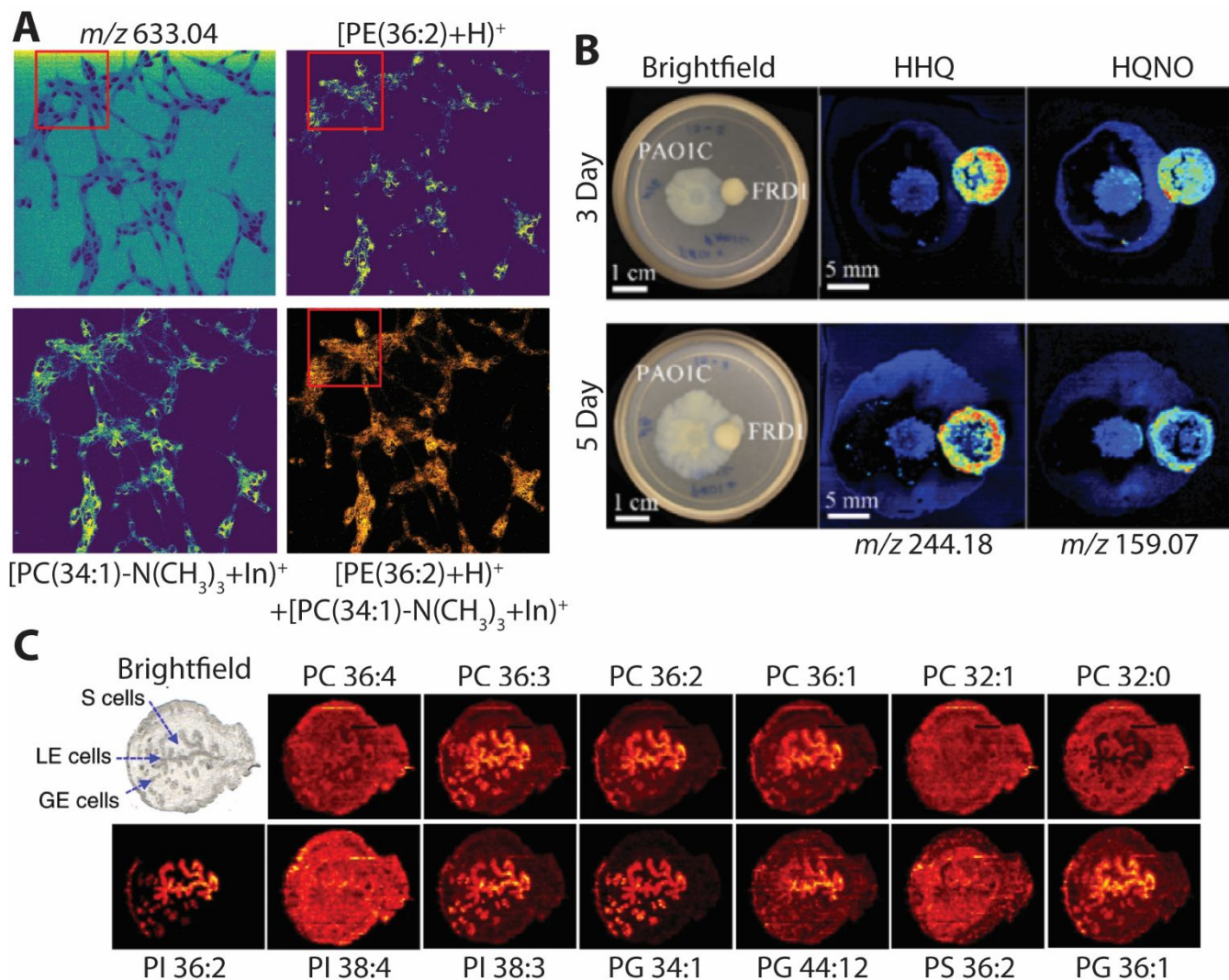


Figure 1. Selected developments within the IMS community. Image of a Vero B cell culture at 1 μm spatial resolution acquired with transition mode MALDI-2 IMS developed by the Dreisewerd lab (A). Panel A is adapted with permission from ref⁴⁷, Niehaus, M. *et al.* *Nat Methods* **16**, 925–931 (2019). Copyright 2019 Nature Publishing. SIMS image of a coculture of different *Pseudomonas aeruginosa* stains visualized with different signaling small molecules (B). Panel B is adapted with permission from ref^{24,48}, Cao, T. *et al.* *SPIE BiOS* **108630A** (2019). Copyright 2019 SPIE. Digital Library. Lipid images both positive and negative mode of the human eye using nanoDESI at 10 μm spatial resolution (C). Panel C is adapted with permission from ref⁴⁹⁻⁵¹, Yin, R. *et al.* *Nature Protocols* **14**, 3445-3470 (2019). Copyright 2019 Nature Publishing.

SIMS utilizes electrostatically focused primary ions (e.g. Bi^+ , Cs^+ , and O^-) or clusters (e.g. Au_3^+ , C_{60} , and Ar) to impact the sample surface, causing a collisional cascade in the top few monolayers of the sample leading to the ejection of secondary ions.^{2,34} Because of the high energy of the ion beam, analyte ions often undergo significant fragmentation and analysis is typically limited to molecular weight ions $< 2 \text{ kDa}$.⁵⁸ The energy of the ion beam plays a critical role in sampling and can be divided into two regimes: static and dynamic SIMS. Static SIMS is defined by low primary ion doses ($< 10^{13} \text{ cm}^{-2}$) and beam currents (pA-nA) suitable for surface analysis of elements and molecules. Alternatively, dynamic SIMS has much higher primary ion doses ($> 10^{13} \text{ cm}^{-2}$) and beam currents (mA), making it suitable for depth profiling and three dimensional imaging.⁵⁹ In general, sample preparation for SIMS analysis is minimal and consists of mounting tissues flatly onto conductive targets and drying prior to introduction into the source vacuum chamber.^{60,61} Although not required, washing samples to remove salts from tissue prior to analysis can improve ion yield.^{62,63}

The primary advantage of SIMS is its high spatial resolution capabilities, because ion beams can be tightly focused using electric fields (1 μm to 30 nm).³² Similar to MALDI, SIMS spatial resolution is defined by the diameter of the ion beam at the surface and the pitch. SIMS has been used for cellular and subcellular analyses,⁶⁴⁻⁶⁷ and for the determination of molecular profiles of various disorders including different cancer types⁶⁸ and cardiovascular disease.⁶⁹ It has also been used to monitor signaling between bacterial cocultures and distinct alkyl quinolone messengers between different stains of *Pseudomonas aeruginosa* (Figure 1B).⁴⁸ Additionally, SIMS was employed to visualize salt redistribution in brain tissue between healthy and stroke mice.⁷⁰ While effective for low molecular weight metabolite and lipid analyses, it has not been commonly applied to peptide and protein imaging studies.

c. Desorption Electrospray Ionization

Desorption electrospray ionization (DESI) is performed by spraying charged solvent droplets on the surface of the sample where the analytes are desorbed and ionized for subsequent detection by MS.⁷¹ The imaging experiment is performed in a continuous raster sampling mode where the target is moved continuously under the DESI spray in a ‘typewriter-like’ motion. Spatial resolution is estimated by the target stage velocity, sampling rate of the mass spectrometer, number of spectra averaged for a single pixel, and distance between adjacent line scans. Although DESI has limited spatial resolution capabilities ($\sim 150 \mu\text{m}$), it requires minimal to no sample preparation. Tissues sections are mounted onto glass slides and sampling is performed at ambient pressure. Recently, the Laskin lab developed a modified form of this sampling approach, termed nanoDESI, using a liquid microjunction to increase spatial resolution to $\sim 10 \mu\text{m}$ (Figure 1C).⁴⁹ While nanoDESI is not discussed in a multimodal imaging context here, we eagerly anticipate the higher spatial resolution of nanoDESI being coupled to other modalities. Moreover, DESI and nanoDESI been used to map metabolite,⁷²⁻⁷⁴ lipid,⁷⁵⁻⁷⁸ and drug distributions in a variety of biological systems ranging from plants to diseased mammalian tissue.⁷⁹⁻⁸¹ Further,

additives in DESI solvent can target specific molecules in the case of reactive DESI⁸² or enhance extraction.⁷²

DESI and nanoDESI IMS are minimally destructive techniques and have been used experimentally in surgical settings to enable intraoperative molecular assessment and aid in real-time intraoperative decisions.^{36,83,84} Sans et al. molecularly characterized high-grade serous carcinoma, serous borderline ovarian tumors and normal ovarian tissue samples using DESI IMS.⁸⁵ They identified predictive markers of cancer aggressiveness and built classification models to enable diagnosis and prediction of high-grade serous carcinoma in comparison to normal tissue with a high certainty of $\sim 96\%$. Similar work from the Eberlin lab has led to the development of a handheld mass spectrometry device, the MasSpec Pen, which enables *in vivo* diagnostics during surgery.^{86,87,88} This device has been used for classifying ovarian⁸⁹ and breast cancer⁹⁰ since it was originally developed. Because it can be operated at atmospheric pressure and requires minimal sample preparation, DESI holds promise for use in clinical and surgical settings.

III. Combining Multiple Imaging Mass Spectrometry Technologies

Since each IMS technology has unique performance characteristics for different molecular classes, there is utility in coupling them together. Technologies such as tandem MS, microextractions, and ion mobility each add additional dimensions to the MS dataset, expanding upon the chemical information that can be obtain, either by enabling *de novo* identification or reducing spectral complexity.

a. Spatially Targeted Tandem MS

Tandem mass spectrometry enables *de novo* identification of molecules within complex samples.⁹¹⁻⁹³ Tandem MS is generally accomplished by performing isolation within one mass analyzer for subsequent fragmentation and transmittance into another mass analyzer for detection.⁹⁴ Serially performing these analyses allows for identification of discrete molecules within a biological sample.^{95,96} In the context of imaging, pixels can be subdivided allowing for a precursor ion scan and subsequent MS/MS scans. This spatially targeted structural information comes at the cost of spatial resolution to accommodate multiple samplings. Additionally, it is often difficult to perform tandem MS analysis within an imaging experiment if the ion of interest is only present within a small number of disperse features or pixels.¹⁷ Alternative means of targeting sample regions or locations for identifying key ions include multimodal image-guided surface sampling,^{97,98} microprobe extraction for offline tandem MS,⁹⁹⁻¹⁰¹ and tandem MS on an orthogonal sample.^{16,30} By using these various strategies, ions that are found in a small number of pixels or structural features can be targeted for analysis.

Tandem MS can be used within an imaging context to identify the differential localization of isomers or isobars within a tissue. Although tandem MS has been reported for several types of IMS technologies,¹⁰²⁻¹⁰⁴ it is primarily used for SIMS imaging because most ion beams fragment analyte ions during the ionization process.¹⁰⁵⁻¹⁰⁹ Any imaging mass spectrometer with MS/MS capabilities can generate fragment ion images^{110,111} enabling direct visualization and differentiation of isomers and isobars within tissue without prior separation or

derivation. Generally, these experiments are usually limited to surveying a small number of ions within a sample, since the tissue is partially consumed during analysis.

b. Multi-Imaging Mass Spectrometry Experiments

Each of the three types of IMS technologies discussed here provide different molecular coverage and spatial resolution. As a result, investigators have combined some of these to gain further functionality. SIMS and MALDI IMS have been combined to detect multiple chemical classes, such as low molecular weight metabolites and lipids within individual cells⁹⁷ and tissue.¹¹³ Additionally, the combination of MALDI and SIMS has been used to analyze hair to enhance sensitivity and spatial resolution.^{114,115} Both MALDI and SIMS sources are operated under vacuum using similar tissue preparation protocols. In some cases, SIMS analyses have been shown to be enhanced by the application of a MALDI matrix.^{116,117} While less common, combining MALDI and DESI together enables analysis of different lipid species,¹¹⁸ and co-mapping of lipids and proteins.¹¹⁹ To our knowledge, there has not yet been a DESI and SIMS multimodal IMS experiment, likely because of the differences in sample preparation. Reaction additives can be employed for DESI analyses for quantitation and derivatization chemistries, bringing additional capabilities to any combination of technologies. Finally, DESI produces multiply charged ions that are often more amenable to tandem MS applications.

c. Microextraction

Microextraction protocols aim to remove key analytes from bulk material to reduce chemical complexity,¹²⁰ and target specific analytes. Both solid and liquid phase extraction techniques have been coupled to IMS for increased peak capacity and sensitivity. Solid phase microextraction (SPME) comprises a diverse set of solventless techniques that allow for *in vivo* analysis. An advantage of SPME devices is that most analytes are introduced into the MS system at once. Introducing ions concurrently increases sensitivity and signal-to-noise (S/N) compared to technologies that generate a transient signal.^{121,122} Furthermore, SPME is used to separate an analyte of interest from bulk material, such as in trace analyte analysis.¹²³

Liquid extractions, such as liquid microjunction (LMJ)^{98,124} and liquid extraction surface analysis (LESA),^{99,125} also enhance peak capacity and reduce ion suppression. Briefly, extraction solvents are dispensed onto a tissue surface and collected for subsequent liquid chromatography or capillary electrophoresis MS analysis.⁵² Spatially targeted liquid extractions are advantageous because they can be coupled to different separation techniques, increasing both sensitivity and depth of coverage. For instance, Cahill et al. used an LMJ to image portions of a microfluidic device while it was functioning with future use aimed at biology-based microfluidic devices.¹²⁶ Typically, this technology utilizes relatively large areas for droplet placement. However, recently microLESA was combined with piezoelectric spotting of trypsin to achieve higher spatial resolution sampling than previously reported.^{99,127} In addition, microLESA was integrated with autofluorescence microscopy to correlate protein signatures of murine kidney and *Staphylococcus aureus* abscesses without tissue staining.⁹⁹ As

these techniques continue to improve in spatial resolution and automated platforms become available, combining IMS with spatially targeted microextractions will be adapted to supplement spatial information with deeper molecular coverage and added identification capabilities.

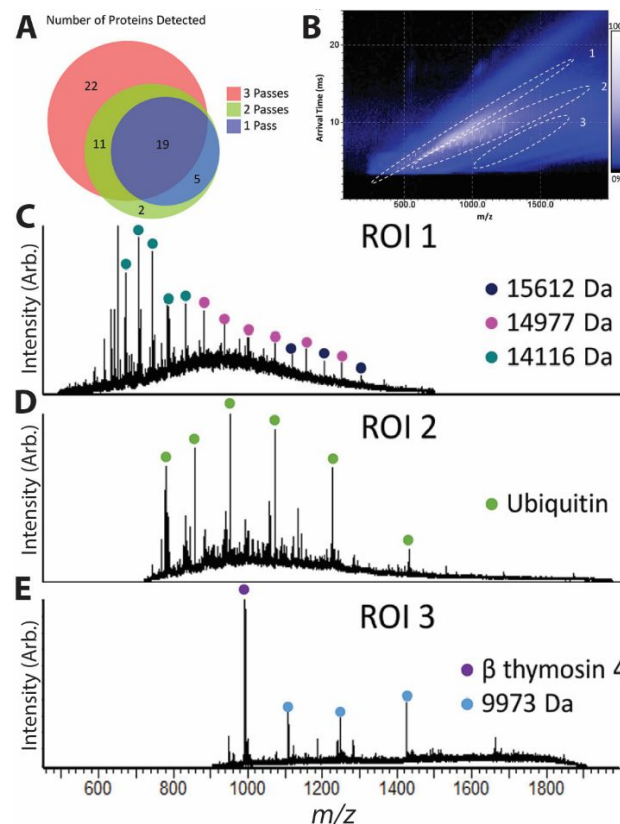


Figure 2. LESA and cIM analysis of a complex murine kidney protein extract. More proteins are detected after each additional cycle of cIM (A). IM heat map generated from a single cycle of cIM (B), where extracted mass spectra from different trend lines contain different protein signatures (C-E). This figure is adapted with permission from ref¹¹², Sisley, E.K. et al. *Analytical Chemistry* (2020). Copyright 2020 American Chemical Society.

d. Ion Mobility

Ion mobility separations add an orthogonal analytical dimension to IMS that reduce ion interference for improving peak capacity and specificity and aiding in identification of species. Additionally, drift time or collision cross sections (CCS) calculated with the use of standards can be used to help identify isomers and isobars. Ion mobility techniques that have been coupled to IMS include drift tube mass spectrometry (DTIMS),^{128,129} traveling wave ion mobility spectrometry (TWIMS),^{130,131} field asymmetric ion mobility spectrometry (FAIMS),¹³²⁻¹³⁴ and—more recently—trapped ion mobility spectrometry (TIMS).¹³⁵⁻¹³⁷

A major focus of the ion mobility field is developing higher resolving power platforms, so they can separate isomers and isobars. Park, Fernandez-Lima, and co-workers utilized a buffer gas and ion trapping by electric field gradient for the development of TIMS devices. They report resolving powers of ~200 but up to ~400.¹³⁸⁻¹⁴⁰ One approach for increasing resolution is by increasing path length and/or number of passes

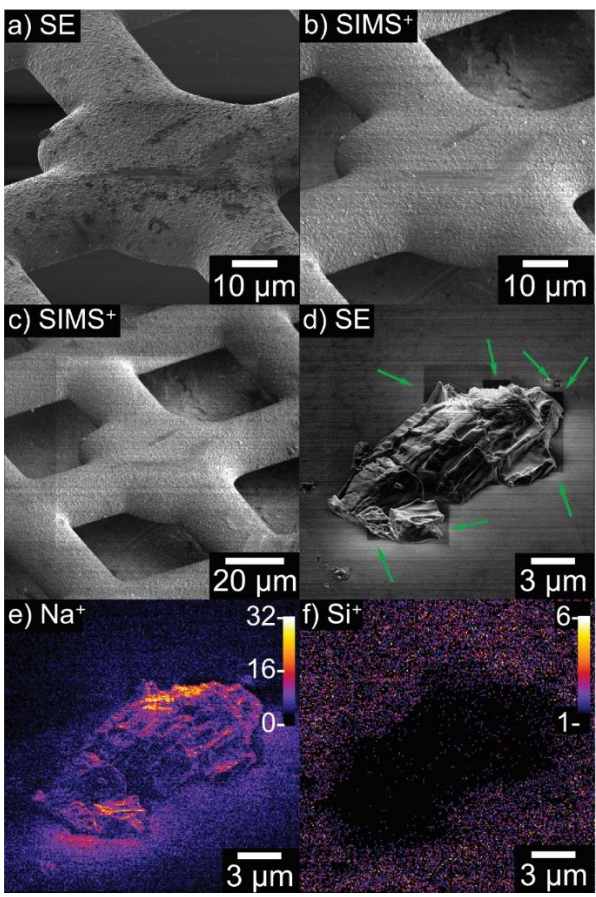


Figure 3. Images of a TEM grid (A-C) and NaCl salt (D-F) crystal generated from the SIMS helium microscope. The SIMS (B,C,E,&F) images are close to the resolution of the microscopy (A&D), demonstrating the power of this technique. This figure is adapted with permission from ref⁴⁹, Klingner, N. *et al.* Ultramicroscopy 198, 10-17 (2019). Copyright 2019 Science Direct.

around the mobility device. Notable ion mobility advancements include the development of structures for lossless ion manipulation (SLIM) devices,^{141,142} as well as the cyclic ion mobility (cIM).¹⁴³ SLIM devices utilize a separation path length of ~540 m¹⁴⁴ for achieving resolving powers over 1800. Using cIM, resolving power of 750 (with 100 passes) has been reported using a reverse sequence peptide pair. Although, sensitivity can be challenging in these devices as ions are lost radially over time. Recently cIM has been integrated with LESA for the improvement of S/N and the number of detected proteins from tissue samples (Figure 2).¹¹²

Beyond increasing peak capacity and specificity, trendlines within ion mobility heat maps can be used to identify different molecular species, classes, and subclasses.¹⁴⁵ For example, MALDI DTIMS IMS was used successfully to separately image a lipid species ([Phosphatidylcholine(34:2)+H⁺]) from a closely isobaric peptide ion (RPPGFSP).¹⁴⁶ Škrášková *et al.* visualized multiply charged polysialylated gangliosides using DESI TWIMS.¹¹⁸ Recently TIMS has been integrated with MALDI IMS to the separate and map isobaric lipid species directly from tissue.¹⁴⁷ Cooper and coworkers introduced a new cylindrical FAIMS device coupled to LESA IMS. This workflow improved the number of detected proteins from what was previously reported

as much as 10 times in murine brain, testes, and kidney.¹⁴⁸ Clearly, ion mobility has great potential for IMS applications as it provides the ability to overcome the analytical challenges associated with direct sampling of complex biological tissues. Software is continually being developed to more efficiently process highly dimensional ion mobility IMS data.

IV. Integration with other technologies

Non-MS analytical technologies can be integrated with MS technologies to increase chemical coverage. Since each technology has distinctive advantages for different molecular classes, experiments that synergistically incorporate multiple technologies gain unique chemical information neither one can obtain alone. For example, many cell types and functional cell states are uniquely suited for analysis by specific methods, such as transcriptomics or immunostaining, and integrating these can add great utility to the molecular specificity of MS.

a. Microscopy

Microscopy is one of the oldest analytical approaches dating back to the early 17th century and is commonly applied to biological and clinical problems.¹⁵⁰⁻¹⁵³ Overall, microscopy images are generated by capturing electromagnetic radiation or particle beams as they interact with the sample through reflection, refraction, or diffraction. A series of lenses and objectives focus the light/particles enabling imaging with high magnification.

Brightfield and histological stains, such as hematoxylin and eosin (H&E) and periodic acid-Schiff (PAS), are used extensively in pathology to assess tissue integrity, health, and disease.¹⁵⁴⁻¹⁵⁶ Stained tissues have been employed with IMS to connect molecular profiles to histological features of both healthy and diseased tissue, such as cancer¹⁵⁷⁻¹⁶¹ and functional disorders.^{162,163} Recently, Basu *et al.* enabled IMS and histology to be rapidly correlated by incorporating matrix pre-coated slides, templates, and a 10 kHz laser.¹⁶⁴ Histological stains are ubiquitous within the scientific and medical field, so multimodal studies that combine IMS and stained microscopy improve interpretation and facilitate collaboration between the technologists and the biologists or physicians. Similarly, simple brightfield images can be used for correlation of IMS signals to specific tissue structures, particularly in cases that have features that are easily distinguished with brightfield microscopy.^{165,166}

Fluorescence microscopy of both endogenous fluorophores^{167,168} and tagged antibodies¹⁶⁹⁻¹⁷¹ or nucleic acids^{172,173} have also been fundamental to our understanding of biological systems. For example, Vardi *et al.* used autofluorescence from chlorophyll and MALDI IMS to study lipid metabolism within algal plaques.¹⁷⁴ By targeting key proteins or genes, investigators can parse metabolic pathways and monitor how these change as a function of disease state or demographic. While exceptionally powerful and informative, these technologies are generally limited to studying peptides or proteins since there are few probes available for low molecular weight metabolites and lipids.^{175,176} IMS has been readily coupled to fluorescence microscopy approaches to tie together cell-type specific immune^{16,17,177,178} and transcript profiles¹⁷⁹⁻¹⁸¹ to metabolites detected by IMS.¹⁸² Immunohistochemistry can be used to histologically classify and contextualize the chemical information obtained by IMS. Moreover, the combination of

both IMS and immunohistochemistry produce more rigorous classification schemes than either modality independently. Recently, several labs have combined immunohistochemistry and IMS to correlate protein or metabolite signals to specific tissue substructures.¹⁸³⁻¹⁸⁶ This type of experiment is further extended by recent work where investigators coupled multiplexed immunohistochemistry with MALDI FT-ICR IMS to determine metabolic profiles of cancer cell, incorporating molecular classes.¹⁸⁷ The increase in the plexity of the immunofluorescence labels additionally enhances the specificity of chemical profiles created by MS analysis, as these immunofluorescence labels can be correlated to more specific tissue regions or cell types.

Immunofluorescence imaging has been correlated with MALDI IMS¹⁷⁸ and fluorescence *in situ* hybridization (FISH) with SIMS.¹⁷⁹ We could not find an example of either being used as part of DESI multimodal studies. This is interesting because there are no experimental considerations preventing IHC or FISH from being combined with all the IMS modalities discussed here. However, technical challenges in co-registering modalities with dramatic differences in spatial resolution may be driving this perceived disparity. Patterson et al. have developed combination experimental and computational pipelines using autofluorescence microscopy to overcome this challenge for multimodal MALDI IMS studies.^{167,168} It is anticipated that fluorescence microscopy will become an important correlative technology in IMS studies.

Particle-based microscopy, such as scanning electron microscopy (SEM) and transmission electron microscopy (TEM), offer very high spatial resolution because it is not diffraction limited. A series of ion optics are used to focus ions towards a sample. The ions then interact with the sample and the emerging electrons and various energy conversion products (e.g. secondary electrons, X-rays, light) are captured as an image. Because nanoSIMS and electron microscopies have similar sample and operational requirements, they have often been used on the same sample.¹⁸⁹ TOF-SIMS has been integrated into a helium ion microscope for 8 nm imaging with the potential for extremely high resolution molecular imaging of biological samples (Figure 3).¹⁴⁹ For example, nanoSIMS and TEM have been combined to map dopamine distributions in dense core vesicles, providing key insight into vesicle loading and nanocompartmentalization.¹⁹⁰ Another study involves integration of fluorescence microscopy, SIMS, high-energy resolution x-ray photoelectron spectroscopy, and SEM on the same plant root to study bacterial growth and infection on this root.¹⁹¹ The authors combined these four modalities because of the simple and compatible sample preparation involved for each. Beyond registration for enhanced localization, particle-based microscopy is also readily used to assess MALDI matrix application for ensuring matrix coverage and crystal size.^{192,193}

b. Spectroscopy

Spectroscopic imaging includes a suite of optical approaches, such as infrared (IR)¹⁹⁴ and Raman, that provide unique spectra of complex chemical mixtures, creating reproducible chemical profiles of different physiological regions and disease states.¹⁹⁵ Spectroscopy is used in a wide array of biological studies,¹⁹⁶⁻²⁰¹ because the approaches are generally non-destructive, label free, and capable of high spatial

resolutions (diffraction limited, 250 nm). While each spectroscopic approach activates different, well characterized molecular modes, it is often difficult to correlate spectroscopic signatures of complex mixtures to discrete chemicals. Rather, they provide general information on bond types and functional groups for the entire chemical mixture.²⁰²⁻²⁰⁵ As such, spectroscopy has been coupled to a variety of MS technologies, including IMS, to provide more detailed molecular descriptions of samples.²⁰⁶⁻²⁰⁸ Because spectroscopic analysis is label free and nondestructive, both modalities can be performed on the same tissue section.²⁰⁹

Raman and IMS have been correlated to study bacteria,²¹⁰⁻²¹² plants,²¹³ single cells,²¹⁴ and mammalian organs.^{215,216} Fourier transform infrared microscopy (FT-IR) has similarly been coupled to IMS for many biological studies.^{209,217,218} Recently, Rabe et al. developed a method for FT-IR guided MALDI IMS (Figure 4). By coupling these two technologies together, the authors reduced data load and acquisition time by >90%.¹⁸⁸ Magnetic resonance imaging has also been used to compliment molecular specificity of IMS with dynamic, whole organ imaging.²¹⁹⁻²²⁴ While MALDI IMS has primarily been coupled to spectroscopic measurements, we foresee DESI increasingly becoming incorporated with Raman and magnetic resonance imaging. DESI does not have many tissue preparation requirements and can theoretically be directly integrated within either approach. Moreover, Raman and magnetic resonance spectra are not saturated when water is

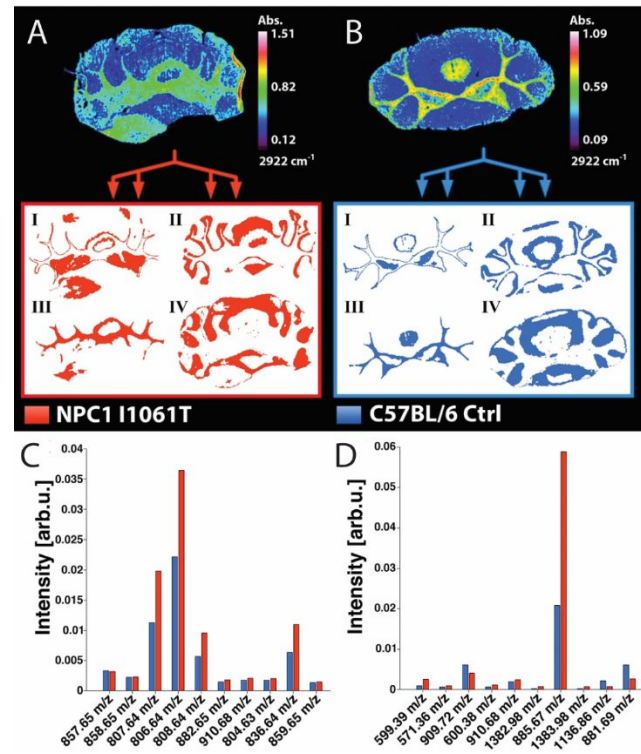


Figure 4. MALDI IMS lipid profiles obtained after FT-IR generated segmentation. Murine brain is differentially segmented based on absorbance of 2922 cm^{-1} based on disease (A) and control mice (B). Using this segmentation, lipid profiles can be generated for different masks for chemical differentiation (C-D). This figure is adapted with permission from ref¹⁸⁸, Rabe, J. A. et al. *Scientific Reports* **8**, 313 (2018). Copyright 2018 Nature Publishing.

present, unlike IR which readily is absorbed by water, making them ideal candidates for multimodal DESI experiments.

c. Transcriptomics

Transcriptomics technologies measure gene expression through the extraction and amplification of nucleic acids, most generally ribonucleic acids.²²⁵⁻²²⁷ Because of the exponential amplification that can occur, this group of technologies are highly sensitive and has been the driving force behind cell typing and classification. There is great interest in coupling IMS with transcriptomics analysis as it would enable simultaneous correlation of gene expression to gene products and biproducts. A majority of the literature combining mass spectrometry and transcriptomics measurements has involved liquid chromatography for bulk proteomics and/or metabolomics.^{228,229} Towards an imaging context, investigators probed an insect, *Carausius morosus*, for neuropeptide content with MALDI MS and correlated this to bulk sequencing to uncover peptides with no known homology.²³⁰ Although this was not an imaging application, the sample preparation was performed in such a way that this workflow could be adapted to an imaging workflow. As an additional step towards combining IMS with transcriptomics, the Knepper et al. microdissected kidney tubules and performed RNA-seq and proteomics.²³¹ This methodology incorporates spatial information of the microdissected structures, which is an important step towards coupling IMS and transcriptomics directly. Moreover, there has been some exciting work where transcriptomics and proteomics IMS information has been correlated on different bulk samples.²³² Work combining two approaches on the same sample provided insight into the link between fatty acids and immunity within breast cancer²³³ and role of liver X receptors in male reproduction.²³⁴ While only a few examples exist, the combination of transcriptomics and IMS will continue to increase in the coming years and has the potential to uncover new connections that span the central dogma of molecular biology.

d. Electrochemistry

Electrochemistry has been vital in the study of electroactive signaling molecules, such as dopamine, epinephrine, serotonin, and histamine within biological systems.²³⁵⁻²³⁷ This is partly because it is capable of absolute quantitation of femto- to zeptomole amounts of analyte at μ s temporal resolutions. It is highly selective and naturally applicable to the analysis of many low molecular weight metabolites, such as neurotransmitters.²³⁸ nanoSIMS/nanoSIMS and electrochemistry are compatible and have been used together often to study nonbiological²³⁹ and biological samples alike.^{238,240,241} Ewing et al. have quantitated L-DOPA concentrations in vesicles and other organelles using nanoSIMS and validated these concentrations with electrochemistry.²⁴² This is particularly important because it enables quantitation of low molecular weight metabolites at high spatial resolutions. Further, Larsson and coworkers quantitated octopamine release during different stimulations using nanoSIMS and an embedded electrode.²⁴³ Investigators in the IMS field have also adapted many technologies and developments from electrochemical studies,²⁴⁴ ranging from nanopipettes to electrochemical principals of ion generation. Adopting materials, analyses, or processes from other fields is

an effective, time saving process that expedites scientific advancements.

V. Future of the Field

Mass spectrometry technologies have rapidly advanced with improved sampling, ion transmission, and detector sensitivity enabling highly sensitive and specific analysis of biological tissues. Under favorable conditions, MS can detect concentrations as low as 10 zeptomoles or approximately 6000 molecules.⁶ This sensitivity is sufficient for probing most molecules within biological systems and yet there is still much we do not understand. Nevertheless, improvements in the molecular, spatial, temporal, and biological specificity are required to answer remaining questions. IMS is one available tool that provides untargeted, highly multiplexed molecular analysis but only through the combination with other technologies can we achieve specificity in all these areas mentioned above. Multimodal imaging experiments can significantly improve performance characteristics including structural identification, throughput, cell type specificity, and dynamic range of MS-based chemical profiles. The present article has summarized the current literature surrounding multimodal IMS and the development of the field to further explore remaining biological questions.

A major task facing multimodal approaches involves efforts to fully integrate the several datasets to enable deeper data mining. This is particularly difficult within an imaging regime because the various technologies can have dramatically different spatial resolutions, data structures, and chemical information. Different computation methods for addressing differences within spatial resolution include various methods of up sampling the data, performing more refined data fusion, as well as other experimental approaches.^{167,168,245-248} While these are capable of connecting modalities that are similar in resolution, significant experimental and technological capabilities are required to avoid the introduction of artifacts.²⁰⁹ While many imaging modalities are within an order of magnitude of one another, this will influence the capacity to combine lower spatial resolution IMS technologies like DESI with higher resolution molecular imaging approaches, like SEM.

Moreover, technologies provide both overlapping and orthogonal information that is often difficult to correlate. For instance, transcriptomics measures gene expression of different biochemical pathways that result with peptide and metabolomic products. Ideally, a highly expressed gene would indicate the presence of a specific metabolite and IMS would detect this same metabolite in high abundance within the same regions, but this is not always the case. There many transport, degradation, and modification pathways that impede this correlation and create complex datasets that are difficult to interpret. Additional compounding technical factors, such as matrix effects, differences in ionization efficiencies, and limited dynamic range add to this complexity. While transcriptomics is used as an example here, a similar scenario applies to other multimodal approaches, such as protein abundances between IMS and immunofluorescence experiments or lipid analysis by Raman spectroscopy and IMS. While challenging, future multimodal experiments will slowly begin to unravel the complex relationships between the data produced by orthogonal technologies. In connection with this, new machine learning

algorithms and approaches will be essential for untangling the abundance of chemical information obtained with multimodal IMS. This will inevitably lead to a more complete picture of biological systems and pathways.

Finally, improving sample preparation and workflows will undoubtedly improve the quality and reproducibility of collected data, particularly as these technologies enter the rigorous domain of medicine and clinical trials. Many technologies cannot be combined “out of the box” and so there are often tradeoffs made to enable multimodal analysis. Although, the gained information from the suboptimal combination of the approaches is often greater than the data of either technique alone. Developing methods that enable multiple imaging modalities to be performed optimally and with minimal spatial compromise will dramatically improve the ability to integrate and discover connections between multimodal datasets. Optimizing the ways and methods behind combining the different approaches is a clear path forward in the field.

In summary, multimodal IMS is a remarkably diverse endeavor that incorporates the best attributes from a variety of scientific disciplines. In the future, multimodal IMS technologies will progressively become more common as the scientific community begins to study more complex biological and medicinal questions. Such studies have the potential to bring together genomic, proteomic, and metabolomic imaging technologies to provide unprecedented insights into biology and medicine.

AUTHOR INFORMATION

Corresponding Author

Jeffery M. Spraggins, Jeff.Spraggins@vanderbilt.edu

Author Contributions

All authors have approved the final version of the manuscript.

ACKNOWLEDGMENTS

Support was provided by the NIH Common Fund and National Institute of Diabetes and Digestive and Kidney Diseases (U54DK120058 awarded to J.M.S. and R.M.C.), NIH National Institute of Allergy and Infectious Disease (R01 AI138581 awarded to J.M.S.), the National Science Foundation Major Research Instrument Program (CBET – 1828299 awarded to J.M.S. and R.M.C.), and by the NIH National Institute of General Medical Sciences (2P41GM103391 awarded to R.M.C.). E.K.N. is supported by a National Institute of Environmental Health Sciences training grant (T32ES007028).

REFERENCES

- (1) Bodzon-Kulakowska, A.; Suder, P. Imaging mass spectrometry: Instrumentation, applications, and combination with other visualization techniques. *Mass Spectrometry Reviews* **2016**, *35*, 147.
- (2) Xu, X.; Zhong, J.; Su, Y.; Zou, Z.; He, Y.; Hou, X. A brief review on mass/optical spectrometry for imaging analysis of biological samples. *Applied Spectroscopy Reviews* **2019**, *54*, 57.
- (3) Ho, Y.-N.; Shu, L.-J.; Yang, Y.-L. Imaging mass spectrometry for metabolites: technical progress, multimodal imaging, and biological interactions. *WIREs Systems Biology and Medicine* **2017**, *9*, e1387.
- (4) Buchberger, A. R.; DeLaney, K.; Johnson, J.; Li, L. Mass Spectrometry Imaging: A Review of Emerging Advancements and Future Insights. *Analytical Chemistry* **2018**, *90*, 240.
- (5) Xu, G.; Li, J. Recent advances in mass spectrometry imaging for multiomics application in neurology. *Journal of Comparative Neurology* **2019**, *527*, 2158.
- (6) Neumann, E. K.; Do, T. D.; Comi, T. J.; Sweedler, J. V. Exploring the Fundamental Structures of Life: Non-Targeted, Chemical Analysis of Single Cells and Subcellular Structures. *Angewandte Chemie International Edition* **2019**, *58*, 9348.
- (7) León, M.; Ferreira, C. R.; Eberlin, L. S.; Jarmusch, A. K.; Pirro, V.; Rodrigues, A. C. B.; Favaron, P. O.; Miglino, M. A.; Cooks, R. G. Metabolites and Lipids Associated with Fetal Swine Anatomy via Desorption Electrospray Ionization – Mass Spectrometry Imaging. *Scientific Reports* **2019**, *9*, 7247.
- (8) Bergman, H.-M.; Lindfors, L.; Palm, F.; Kihlberg, J.; Lanekoff, I. Metabolite aberrations in early diabetes detected in rat kidney using mass spectrometry imaging. *Analytical and Bioanalytical Chemistry* **2019**, *411*, 2809.
- (9) Morse, N.; Jamaspishvili, T.; Simon, D.; Patel, P. G.; Ren, K. Y. M.; Wang, J.; Oleschuk, R.; Kaufmann, M.; Gooding, R. J.; Berman, D. M. Reliable identification of prostate cancer using mass spectrometry metabolomic imaging in needle core biopsies. *Laboratory Investigation* **2019**, *99*, 1561.
- (10) Wang, M.; Dubiak, K.; Zhang, Z.; Huber, P. W.; Chen, D. D. Y.; Dovichi, N. J. MALDI-imaging of early stage Xenopus laevis embryos. *Talanta* **2019**, *204*, 138.
- (11) Shariatgorji, M.; Nilsson, A.; Fridjonsdottir, E.; Vallianatou, T.; Källback, P.; Katan, L.; Sävmarkar, J.; Mantas, I.; Zhang, X.; Bezard, E.; Svensson, P.; Odell, L. R.; Andrén, P. E. Comprehensive mapping of neurotransmitter networks by MALDI-MS imaging. *Nature Methods* **2019**, *16*, 1021.
- (12) Watrous, J. D.; Dorrestein, P. C. Imaging mass spectrometry in microbiology. *Nature Reviews Microbiology* **2011**, *9*, 683.
- (13) Shank, E. A.; Kolter, R. Extracellular signaling and multicellularity in *Bacillus subtilis*. *Current opinion in microbiology* **2011**, *14*, 741.
- (14) Alamri, H.; Patterson, N. H.; Yang, E.; Zoroquiain, P.; Lazaris, A.; Chaurand, P.; Metrakos, P. Mapping the triglyceride distribution in NAFLD human liver by MALDI imaging mass spectrometry reveals molecular differences in micro and macro steatosis. *Analytical and Bioanalytical Chemistry* **2019**, *411*, 885.
- (15) Sämfors, S.; Fletcher, J. S. Lipid Diversity in Cells and Tissue Using Imaging SIMS. *Annual Review of Analytical Chemistry* **2020**, *13*, null.
- (16) Neumann, E. K.; Comi, T. J.; Rubakhin, S. S.; Sweedler, J. V. Lipid Heterogeneity between Astrocytes and Neurons Revealed by Single-Cell MALDI-MS Combined with Immunocytochemical Classification. *Angewandte Chemie International Edition* **2019**, *58*, 5910.
- (17) Neumann, E. K.; Ellis, J. F.; Triplett, A. E.; Rubakhin, S. S.; Sweedler, J. V. Lipid Analysis of 30 000 Individual Rodent Cerebellar Cells Using High-Resolution Mass Spectrometry. *Analytical Chemistry* **2019**, *91*, 7871.
- (18) Nemes, P.; Woods, A. S.; Vertes, A. Simultaneous Imaging of Small Metabolites and Lipids in Rat Brain Tissues at Atmospheric Pressure by Laser Ablation Electrospray Ionization Mass Spectrometry. *Analytical Chemistry* **2010**, *82*, 982.
- (19) Eberlin, L. S.; Dill, A. L.; Golby, A. J.; Ligon, K. L.; Wiseman, J. M.; Cooks, R. G.; Agar, N. Y. R. Discrimination of Human Astrocytoma Subtypes by Lipid Analysis Using Desorption Electrospray Ionization Mass Spectrometry. *Angewandte Chemie International Edition* **2010**, *49*, 5953.
- (20) Angel, P. M.; Spraggins, J. M.; Baldwin, H. S.; Caprioli, R. Enhanced sensitivity for high spatial resolution lipid analysis by negative ion mode matrix assisted laser desorption ionization imaging mass spectrometry. *Analytical Chemistry* **2012**, *84*, 1557.
- (21) Brunelle, A.; Laprévote, O. Lipid imaging with cluster time-of-flight secondary ion mass spectrometry. *Analytical and Bioanalytical Chemistry* **2009**, *393*, 31.
- (22) Rešetar Maslov, D.; Svirčová, A.; Allmaier, G.; Marchetti-Deschamann, M.; Kraljević Pavelić, S. Optimization of MALDI-TOF mass spectrometry imaging for the visualization and comparison of peptide distributions in dry-cured ham muscle fibers. *Food Chemistry* **2019**, *283*, 275.

(23) Do, T. D.; Ellis, J. F.; Neumann, E. K.; Comi, T. J.; Tillmaand, E. G.; Lenhart, A. E.; Rubakhin, S. S.; Sweedler, J. V. Optically Guided Single Cell Mass Spectrometry of Rat Dorsal Root Ganglia to Profile Lipids, Peptides and Proteins. *ChemPhysChem* **2018**, *19*, 1180.

(24) Caprioli, R. M.; Farmer, T. B.; Gile, J. Molecular Imaging of Biological Samples: Localization of Peptides and Proteins Using MALDI-TOF MS. *Analytical Chemistry* **1997**, *69*, 4751.

(25) Dilillo, M.; Ait-Belkacem, R.; Esteve, C.; Pellegrini, D.; Nicolardi, S.; Costa, M.; Vannini, E.; Graaf, E. L. d.; Caleo, M.; McDonnell, L. A. Ultra-High Mass Resolution MALDI Imaging Mass Spectrometry of Proteins and Metabolites in a Mouse Model of Glioblastoma. *Scientific Reports* **2017**, *7*, 603.

(26) Garza, K. Y.; Feider, C. L.; Klein, D. R.; Rosenberg, J. A.; Brodbelt, J. S.; Eberlin, L. S. Desorption Electrospray Ionization Mass Spectrometry Imaging of Proteins Directly from Biological Tissue Sections. *Analytical Chemistry* **2018**, *90*, 7785.

(27) Andersson, M.; Groseclose, M. R.; Deutch, A. Y.; Caprioli, R. M. Imaging mass spectrometry of proteins and peptides: 3D volume reconstruction. *Nature Methods* **2008**, *5*, 101.

(28) Groseclose, M. R.; Andersson, M.; Hardesty, W. M.; Caprioli, R. M. Identification of proteins directly from tissue: in situ tryptic digestions coupled with imaging mass spectrometry. *Journal of Mass Spectrometry* **2007**, *42*, 254.

(29) Crecelius, A. C.; Cornett, D. S.; Caprioli, R. M.; Williams, B.; Dawant, B. M.; Bodenheimer, B. Three-dimensional visualization of protein expression in mouse brain structures using imaging mass spectrometry. *Journal of The American Society for Mass Spectrometry* **2005**, *16*, 1093.

(30) Ryan, D. J.; Spraggins, J. M.; Caprioli, R. M. Protein identification strategies in MALDI imaging mass spectrometry: a brief review. *Current Opinion in Chemical Biology* **2019**, *48*, 64.

(31) Angeletti, S.; Ciccozzi, M. Matrix-assisted laser desorption ionization time-of-flight mass spectrometry in clinical microbiology: An updating review. *Infection, Genetics and Evolution* **2019**, *76*, 104063.

(32) Eswara, S.; Pshenova, A.; Yedra, L.; Hoang, Q. H.; Lovric, J.; Philipp, P.; Wirtz, T. Correlative microscopy combining transmission electron microscopy and secondary ion mass spectrometry: A general review on the state-of-the-art, recent developments, and prospects. *Applied Physics Reviews* **2019**, *6*, 021312.

(33) Gyngard, F.; Steinhauser, M. L. Biological explorations with nanoscale secondary ion mass spectrometry. *Journal of Analytical Atomic Spectrometry* **2019**, *34*, 1534.

(34) Gao, D.; Huang, X.; Tao, Y. A critical review of NanoSIMS in analysis of microbial metabolic activities at single-cell level. *Critical Reviews in Biotechnology* **2016**, *36*, 884.

(35) Zheng, Q.; Chen, H. Development and Applications of Liquid Sample Desorption Electrospray Ionization Mass Spectrometry. *Annual Review of Analytical Chemistry* **2016**, *9*, 411.

(36) Ferreira, C.; Alfaro, C. M.; Pirro, V.; Cooks, R. G. Desorption Electrospray Ionization Mass Spectrometry Imaging: Recent Developments and Perspectives. *J Biomol Tech* **2019**, *30*, S46.

(37) Javanshad, R.; Venter, A. R. Ambient ionization mass spectrometry: real-time, proximal sample processing and ionization. *Analytical Methods* **2017**, *9*, 4896.

(38) Parrot, D.; Papazian, S.; Foil, D.; Tasdemir, D. Imaging the Unimaginable: Desorption Electrospray Ionization – Imaging Mass Spectrometry (DESI-IMS) in Natural Product Research. *Planta Med* **2018**, *84*, 584.

(39) Shrestha, B.; Walsh, C. M.; Boyce, G. R.; Nemes, P. In *Advances in MALDI and Laser-Induced Soft Ionization Mass Spectrometry*; Springer: 2016, p 149.

(40) In *Proteomics for Biological Discovery*, p 89.

(41) Strupat, K.; Karas, M.; Hillenkamp, F. 2,5-Dihydroxybenzoic acid: a new matrix for laser desorption–ionization mass spectrometry. *International Journal of Mass Spectrometry and Ion Processes* **1991**, *111*, 89.

(42) Beavis, R. C.; Chaudhary, T.; Chait, B. T. α -Cyno-4-hydroxycinnamic acid as a matrix for matrixassisted laser desorption mass spectromtry. *Organic Mass Spectrometry* **1992**, *27*, 156.

(43) Vermillion-Salsbury, R. L.; Hercules, D. M. 9-Aminoacridine as a matrix for negative mode matrix-assisted laser desorption/ionization. *Rapid Communications in Mass Spectrometry* **2002**, *16*, 1575.

(44) Korte, A. R.; Lee, Y. J. MALDI-MS analysis and imaging of small molecule metabolites with 1,5-diaminonaphthalene (DAN). *Journal of Mass Spectrometry* **2014**, *49*, 737.

(45) Scott, A. J.; Flinders, B.; Cappell, J.; Liang, T.; Pelc, R. S.; Tran, B.; Kilgour, D. P. A.; Heeren, R. M. A.; Goodlett, D. R.; Ernst, R. K. Norharmane matrix enhances detection of endotoxin by MALDI-MS for simultaneous profiling of pathogen, host and vector systems. *Pathogens and Disease* **2016**, *74*.

(46) Amstalden van Hove, E. R.; Smith, D. F.; Heeren, R. M. A. A concise review of mass spectrometry imaging. *Journal of Chromatography A* **2010**, *1217*, 3946.

(47) Niehaus, M.; Soltwisch, J.; Belov, M. E.; Dreisewerd, K. Transmission-mode MALDI-2 mass spectrometry imaging of cells and tissues at subcellular resolution. *Nature Methods* **2019**, *16*, 925.

(48) Cao, T.; Morales-Soto, N.; Jia, J.; Baig, N.; Dunham, S. J.; Ellis, J.; Sweedler, J.; Shrout, J.; Bohn, P. *Spatiotemporal dynamics of molecular messaging in bacterial co-cultures studied by multimodal chemical imaging*; SPIE, 2019; Vol. 10863.

(49) Yin, R.; Burnum-Johnson, K. E.; Sun, X.; Dey, S. K.; Laskin, J. High spatial resolution imaging of biological tissues using nanospray desorption electrospray ionization mass spectrometry. *Nature Protocols* **2019**, *14*, 3445.

(50) Cornett, D. S.; Frappier, S. L.; Caprioli, R. M. MALDI-FTICR Imaging Mass Spectrometry of Drugs and Metabolites in Tissue. *Analytical Chemistry* **2008**, *80*, 5648.

(51) Greer, T.; Sturm, R.; Li, L. Mass spectrometry imaging for drugs and metabolites. *Journal of Proteomics* **2011**, *74*, 2617.

(52) Boughton, B. A.; Thinagaran, D.; Sarabia, D.; Bacic, A.; Roessner, U. Mass spectrometry imaging for plant biology: a review. *Phytochemistry Reviews* **2016**, *15*, 445.

(53) Trim, P. J.; Snel, M. F. Small molecule MALDI MS imaging: Current technologies and future challenges. *Methods* **2016**, *104*, 127.

(54) Murray, K. K.; Seneviratne, C. A.; Ghorai, S. High resolution laser mass spectrometry bioimaging. *Methods* **2016**, *104*, 118.

(55) Heiles, S.; Kompauer, M.; Müller, M. A.; Spengler, B. Atmospheric-Pressure MALDI Mass Spectrometry Imaging at 213 nm Laser Wavelength. *Journal of The American Society for Mass Spectrometry* **2020**, *31*, 326.

(56) Zavalin, A.; Yang, J.; Hayden, K.; Vestal, M.; Caprioli, R. M. Tissue protein imaging at 1 μ m laser spot diameter for high spatial resolution and high imaging speed using transmission geometry MALDI TOF MS. *Analytical and Bioanalytical Chemistry* **2015**, *407*, 2337.

(57) Spivey, E. C.; McMillen, J. C.; Ryan, D. J.; Spraggins, J. M.; Caprioli, R. M. Combining MALDI-2 and transmission geometry laser optics to achieve high sensitivity for ultra-high spatial resolution surface analysis. *Journal of Mass Spectrometry* **2019**, *54*, 366.

(58) Wogrel, L.; Höök, F.; Agnarsson, B.; Sjövall, P. Toward multiplexed quantification of biomolecules on surfaces using time-of-flight secondary ion mass spectrometry. *Biointerphases* **2018**, *13*, 03B413.

(59) Sodhi, R. N. S. Time-of-flight secondary ion mass spectrometry (TOF-SIMS)—versatility in chemical and imaging surface analysis. *Analyst* **2004**, *129*, 483.

(60) Yoon, S.; Lee, T. G. Biological tissue sample preparation for time-of-flight secondary ion mass spectrometry (ToF-SIMS) imaging. *Nano Convergence* **2018**, *5*, 24.

(61) Schaepe, K.; Jungnickel, H.; Heinrich, T.; Tentschert, J.; Luch, A.; Unger, W. E. S. In *Characterization of Nanoparticles*; Hodoroaba, V.-D., Unger, W. E. S., Shard, A. G., Eds.; Elsevier: 2020, p 481.

(62) Gilmore, I. S.; Heiles, S.; Pieterse, C. L. Metabolic Imaging at the Single-Cell Scale: Recent Advances in Mass Spectrometry Imaging. *Annual Review of Analytical Chemistry* **2019**, *12*, 201.

(63) Nuñez, J.; Renslow, R.; CliffIII, J. B.; Anderton, C. R. NanoSIMS for biological applications: Current practices and analyses. *Biointerphases* **2018**, *13*, 03B301.

(64) Tian, H.; Six, D. A.; Krucker, T.; Leeds, J. A.; Winograd, N. Subcellular Chemical Imaging of Antibiotics in Single Bacteria Using C60-Secondary Ion Mass Spectrometry. *Analytical Chemistry* **2017**, *89*, 5050.

(65) Massonnet, P.; Heeren, R. M. A. A concise tutorial review of TOF-SIMS based molecular and cellular imaging. *Journal of Analytical Atomic Spectrometry* **2019**, *34*, 2217.

(66) Yin, L.; Zhang, Z.; Liu, Y.; Gao, Y.; Gu, J. Recent advances in single-cell analysis by mass spectrometry. *Analyst* **2019**, *144*, 824.

(67) Li, H.-W.; Hua, X.; Long, Y.-T. Graphene quantum dots enhanced ToF-SIMS for single-cell imaging. *Analytical and Bioanalytical Chemistry* **2019**, *411*, 4025.

(68) Gulyaryan, S. K.; Gulin, A. A.; Anufrieva, K. S.; Shender, V.; Shakhpasov, M. I.; Bastola, S.; Antipova, N. V.; Kovalenko, T. F.; Rubtsov, Y. P.; Latyshev, Y. A.; Potapov, A. A.; Pavlyukov, M. S. Investigation of inter- and intra-tumoral heterogeneity of glioblastoma using TOF-SIMS. *Molecular & Cellular Proteomics* **2020**, mcp.RA120.001986.

(69) Mezger, S. T. P.; Mingels, A. M. A.; Bekers, O.; Cillero-Pastor, B.; Heeren, R. M. A. Trends in mass spectrometry imaging for cardiovascular diseases. *Analytical and Bioanalytical Chemistry* **2019**, *411*, 3709.

(70) Mulder, I. A.; Ogrinc Potočnik, N.; Broos, L. A. M.; Prop, A.; Wermer, M. J. H.; Heeren, R. M. A.; van den Maagdenberg, A. M. J. M. Distinguishing core from penumbra by lipid profiles using Mass Spectrometry Imaging in a transgenic mouse model of ischemic stroke. *Scientific Reports* **2019**, *9*, 1090.

(71) Wiseman, J. M.; Ifa, D. R.; Venter, A.; Cooks, R. G. Ambient molecular imaging by desorption electrospray ionization mass spectrometry. *Nature Protocols* **2008**, *3*, 517.

(72) Wang, X.; Hou, Y.; Hou, Z.; Xiong, W.; Huang, G. Mass Spectrometry Imaging of Brain Cholesterol and Metabolites with Trifluoroacetic Acid-Enhanced Desorption Electrospray Ionization. *Analytical Chemistry* **2019**, *91*, 2719.

(73) Huang, L.; Mao, X.; Sun, C.; Luo, Z.; Song, X.; Li, X.; Zhang, R.; Lv, Y.; Chen, J.; He, J.; Abiliz, Z. A graphical data processing pipeline for mass spectrometry imaging-based spatially resolved metabolomics on tumor heterogeneity. *Analytica Chimica Acta* **2019**, *1077*, 183.

(74) Martin, R.; Midey, A.; Olivos, H.; Shrestha, B.; Claude, E. Spatial Mapping of Lipids and Neurotransmitters in Rat Brain Section Using DESI Ion Mobility Mass Spectrometry. *J Biomol Tech* **2019**, *30*, S38.

(75) Nguyen, S. N.; Kyle, J. E.; Dautel, S. E.; Sontag, R.; Luders, T.; Corley, R.; Ansong, C.; Carson, J.; Laskin, J. Lipid Coverage in Nanospray Desorption Electrospray Ionization Mass Spectrometry Imaging of Mouse Lung Tissues. *Analytical Chemistry* **2019**, *91*, 11629.

(76) Nagai, K.; Uranbileg, B.; Chen, Z.; Fujioka, A.; Yamazaki, T.; Matsumoto, Y.; Tsukamoto, H.; Ikeda, H.; Yatomi, Y.; Chiba, H.; Hui, S.-P.; Nakazawa, T.; Saito, R.; Koshiba, S.; Aoki, J.; Saigusa, D.; Tomioka, Y. Identification of novel biomarkers of hepatocellular carcinoma by high-definition mass spectrometry: Ultrahigh-performance liquid chromatography quadrupole time-of-flight mass spectrometry and desorption electrospray ionization mass spectrometry imaging. *Rapid Communications in Mass Spectrometry* **2020**, *34*, e8551.

(77) Liu, C.; Qi, K.; Yao, L.; Xiong, Y.; Zhang, X.; Zang, J.; Tian, C.; Xu, M.; Yang, J.; Lin, Z.; Lv, Y.; Xiong, W.; Pan, Y. Imaging of Polar and Nonpolar Species Using Compact Desorption Electrospray Ionization/Postphotoionization Mass Spectrometry. *Analytical Chemistry* **2019**, *91*, 6616.

(78) Unsihay, D.; Qiu, J.; Swaroop, S.; Nagornov, K. O.; Kozhinov, A. N.; Tsybin, Y. O.; Kuang, S.; Laskin, J. Imaging of triglycerides in tissues using nanospray desorption electrospray ionization (Nano-DESI) mass spectrometry. *International Journal of Mass Spectrometry* **2020**, *448*, 116269.

(79) Feider, C. L.; Woody, S.; Ledet, S.; Zhang, J.; Sebastian, K.; Breen, M. T.; Eberlin, L. S. Molecular Imaging of Endometriosis Tissues using Desorption Electrospray Ionization Mass Spectrometry. *Scientific Reports* **2019**, *9*, 15690.

(80) Banerjee, S.; Wong, A. C.-Y.; Yan, X.; Wu, B.; Zhao, H.; Tibshirani, R. J.; Zare, R. N.; Brooks, J. D. Early detection of unilateral ureteral obstruction by desorption electrospray ionization mass spectrometry. *Scientific Reports* **2019**, *9*, 11007.

(81) Tamura, K.; Horikawa, M.; Sato, S.; Miyake, H.; Setou, M. Discovery of lipid biomarkers correlated with disease progression in clear cell renal cell carcinoma using desorption electrospray ionization imaging mass spectrometry. *Oncotarget* **2019**, *10*, 1688.

(82) Zheng, Q.; Ruan, X.; Tian, Y.; Hu, J.; Wan, N.; Lu, W.; Xu, X.; Wang, G.; Hao, H.; Ye, H. Ligand–protein target screening from cell matrices using reactive desorption electrospray ionization–mass spectrometry via a native-denatured exchange approach. *Analyst* **2019**, *144*, 512.

(83) Alfaro, C. M.; Pirro, V.; Keating, M. F.; Hattab, E. M.; Cooks, R. G.; Cohen-Gadol, A. A. Intraoperative assessment of isocitrate dehydrogenase mutation status in human gliomas using desorption electrospray ionization–mass spectrometry. *2019*, *132*, 180.

(84) DeHoog, R. J.; Zhang, J.; Alore, E.; Lin, J. Q.; Yu, W.; Woody, S.; Almendariz, C.; Lin, M.; Engelsman, A. F.; Sidhu, S. B.; Tibshirani, R.; Suliburk, J.; Eberlin, L. S. Preoperative metabolic classification of thyroid nodules using mass spectrometry imaging of fine-needle aspiration biopsies. *Proceedings of the National Academy of Sciences* **2019**, *116*, 21401.

(85) Sans, M.; Gharpure, K.; Tibshirani, R.; Zhang, J.; Liang, L.; Liu, J.; Young, J. H.; Dood, R. L.; Sood, A. K.; Eberlin, L. S. Metabolic Markers and Statistical Prediction of Serous Ovarian Cancer Aggressiveness by Ambient Ionization Mass Spectrometry Imaging. *Cancer Research* **2017**, *77*, 2903.

(86) Zhang, J.; Rector, J.; Lin, J. Q.; Young, J. H.; Sans, M.; Katta, N.; Giese, N.; Yu, W.; Nagi, C.; Suliburk, J.; Liu, J.; Bensussan, A.; DeHoog, R. J.; Garza, K. Y.; Ludolph, B.; Sorace, A. G.; Syed, A.; Zahedivash, A.; Milner, T. E.; Eberlin, L. S. Nondestructive tissue analysis for ex vivo and in vivo cancer diagnosis using a handheld mass spectrometry system. *Science Translational Medicine* **2017**, *9*, eaan3968.

(87) Feider, C. L.; Krieger, A.; DeHoog, R. J.; Eberlin, L. S. Ambient Ionization Mass Spectrometry: Recent Developments and Applications. *Analytical Chemistry* **2019**, *91*, 4266.

(88) Hall, O. M.; Peer, C. J.; Figg, W. D. Tissue preservation with mass spectroscopic analysis: Implications for cancer diagnostics. *Cancer Biol Ther* **2018**, *19*, 953.

(89) Sans, M.; Zhang, J.; Lin, J. Q.; Feider, C. L.; Giese, N.; Breen, M. T.; Sebastian, K.; Liu, J.; Sood, A. K.; Eberlin, L. S. Performance of the MasSpec Pen for Rapid Diagnosis of Ovarian Cancer. *Clinical Chemistry* **2019**, *65*, 674.

(90) St John, E. R.; Balog, J.; McKenzie, J. S.; Rossi, M.; Covington, A.; Muirhead, L.; Bodai, Z.; Rosini, F.; Speller, A. V.; Shousha, S. Rapid evaporative ionisation mass spectrometry of electrosurgical vapours for the identification of breast pathology: towards an intelligent knife for breast cancer surgery. *Breast Cancer Research* **2017**, *19*, 59.

(91) Tran, N. H.; Zhang, X.; Xin, L.; Shan, B.; Li, M. De novo peptide sequencing by deep learning. *Proceedings of the National Academy of Sciences* **2017**, *114*, 8247.

(92) Kumar, D.; Yadav, A. K.; Dash, D. In *Proteome Bioinformatics*; Springer: 2017, p 17.

(93) Jadid, S. E.; Touahni, R.; Moussa, A. In *Proceedings of the New Challenges in Data Sciences: Acts of the Second Conference of the Moroccan Classification Society*; Association for Computing Machinery: Kenitra, Morocco, 2019, p Article 4.

(94) El-Aneed, A.; Cohen, A.; Banoub, J. Mass Spectrometry, Review of the Basics: Electrospray, MALDI, and Commonly Used Mass Analyzers. *Applied Spectroscopy Reviews* **2009**, *44*, 210.

(95) Korte, A. R.; Yagnik, G. B.; Feenstra, A. D.; Lee, Y. J. Multiplex MALDI-MS imaging of plant metabolites using a hybrid MS system. *Methods Mol Biol* **2015**, *1203*, 49.

(96) Ellis, S. R.; Paine, M. R. L.; Eijkel, G. B.; Pauling, J. K.; Husen, P.; Jervelund, M. W.; Hermansson, M.; Ejsing, C. S.; Heeren, R. M. A. Automated, parallel mass spectrometry imaging and structural identification of lipids. *Nature Methods* **2018**, *15*, 515.

(97) Comi, T. J.; Neumann, E. K.; Do, T. D.; Sweedler, J. V. microMS: A Python Platform for Image-Guided Mass Spectrometry Profiling. *Journal of the American Society for Mass Spectrometry* **2017**, *28*, 1919.

(98) Comi, T. J.; Makurath, M. A.; Philip, M. C.; Rubakhin, S. S.; Sweedler, J. V. MALDI MS Guided Liquid Microjunction Extraction for Capillary Electrophoresis–Electrospray Ionization MS Analysis of Single Pancreatic Islet Cells. *Analytical Chemistry* **2017**, *89*, 7765.

(99) Ryan, D. J.; Patterson, N. H.; Putnam, N. E.; Wilde, A. D.; Weiss, A.; Perry, W. J.; Cassat, J. E.; Skaar, E. P.; Caprioli, R. M.;

Spraggins, J. M. MicroLESA: Integrating Autofluorescence Microscopy, In Situ Micro-Digestions, and Liquid Extraction Surface Analysis for High Spatial Resolution Targeted Proteomic Studies. *Analytical Chemistry* **2019**, *91*, 7578.

(100) Ryan, D. J.; Nei, D.; Prentice, B. M.; Rose, K. L.; Caprioli, R. M.; Spraggins, J. M. Protein identification in imaging mass spectrometry through spatially targeted liquid micro-extractions. *Rapid Communications in Mass Spectrometry* **2018**, *32*, 442.

(101) Delcourt, V.; Franck, J.; Quanico, J.; Gimeno, J.-P.; Wisztorski, M.; Raffo-Romero, A.; Kobeissy, F.; Roucou, X.; Salzet, M.; Fournier, I. Spatially-Resolved Top-down Proteomics Bridged to MALDI MS Imaging Reveals the Molecular Physiome of Brain Regions. *Molecular & Cellular Proteomics* **2018**, *17*, 357.

(102) Kompauer, M.; Heiles, S.; Spengler, B. Atmospheric pressure MALDI mass spectrometry imaging of tissues and cells at 1.4- μ m lateral resolution. *Nature Methods* **2017**, *14*, 90.

(103) Prentice, B. M.; McMullen, J. C.; Caprioli, R. M. Multiple TOF/TOF events in a single laser shot for multiplexed lipid identifications in MALDI imaging mass spectrometry. *International Journal of Mass Spectrometry* **2019**, *437*, 30.

(104) Pasilis, S. P.; Kertesz, V.; Van Berkel, G. J.; Schulz, M.; Schorcht, S. HPTLC/DESI-MS imaging of tryptic protein digests separated in two dimensions. *Journal of Mass Spectrometry* **2008**, *43*, 1627.

(105) Fisher, G. L. Structural Assessment of (Sub-)Monolayer Coatings in Device Processing at High Spatial Resolving Power by TOF-SIMS Tandem MS Imaging. *Microscopy and Microanalysis* **2019**, *25*, 732.

(106) Angerer, T. B.; Velickovic, D.; Nicora, C. D.; Kyle, J. E.; Graham, D. J.; Anderton, C.; Gamble, L. J. Exploiting the Semidestructive Nature of Gas Cluster Ion Beam Time-of-Flight Secondary Ion Mass Spectrometry Imaging for Simultaneous Localization and Confident Lipid Annotations. *Analytical Chemistry* **2019**, *91*, 15073.

(107) Bruinen, A. L.; Fisher, G. L.; Heeren, R. M. In *Imaging Mass Spectrometry*; Springer: 2017, p 165.

(108) Ogrinc Potočnik, N.; Fisher, G. L.; Prop, A.; Heeren, R. M. A. Sequencing and Identification of Endogenous Neuropeptides with Matrix-Enhanced Secondary Ion Mass Spectrometry Tandem Mass Spectrometry. *Analytical Chemistry* **2017**, *89*, 8223.

(109) Fu, T.; Houél, E.; Amusant, N.; Touboul, D.; Genta-Jouve, G.; Della-Negra, S.; Fisher, G. L.; Brunelle, A.; Duplais, C. Biosynthetic investigation of γ -lactones in *Sextonia rubra* wood using in situ TOF-SIMS MS/MS imaging to localize and characterize biosynthetic intermediates. *Scientific Reports* **2019**, *9*, 1928.

(110) Sugiura, Y.; Zaima, N.; Setou, M.; Ito, S.; Yao, I. Visualization of acetylcholine distribution in central nervous system tissue sections by tandem imaging mass spectrometry. *Analytical and Bioanalytical Chemistry* **2012**, *403*, 1851.

(111) Takeo, E.; Sugiura, Y.; Uemura, T.; Nishimoto, K.; Yasuda, M.; Sugiyama, E.; Ohtsuki, S.; Higashi, T.; Nishikawa, T.; Suematsu, M.; Fukusaki, E.; Shimma, S. Tandem Mass Spectrometry Imaging Reveals Distinct Accumulation Patterns of Steroid Structural Isomers in Human Adrenal Glands. *Analytical Chemistry* **2019**, *91*, 8918.

(112) Sisley, E. K.; Ujma, J.; Palmer, M.; Giles, K.; Fernandez-Lima, F. A.; Cooper, H. J. LESA Cyclic Ion Mobility Mass Spectrometry of Intact Proteins from Thin Tissue Sections. *Analytical Chemistry* **2020**.

(113) Desbenoit, N.; Walch, A.; Spengler, B.; Brunelle, A.; Römpf, A. Correlative mass spectrometry imaging, applying time-of-flight secondary ion mass spectrometry and atmospheric pressure matrix-assisted laser desorption/ionization to a single tissue section. *Rapid Communications in Mass Spectrometry* **2018**, *32*, 159.

(114) Erne, R.; Bernard, L.; Steuer, A. E.; Baumgartner, M. R.; Kraemer, T. Hair Analysis: Contamination versus Incorporation from the Circulatory System—Investigations on Single Hair Samples Using Time-of-Flight Secondary Ion Mass Spectrometry and Matrix-Assisted Laser Desorption/Ionization Mass Spectrometry. *Analytical Chemistry* **2019**, *91*, 4132.

(115) Lanni, E. J.; Masyuko, R. N.; Driscoll, C. M.; Aerts, J. T.; Shroud, J. D.; Bohn, P. W.; Sweedler, J. V. MALDI-guided SIMS: Multiscale Imaging of Metabolites in Bacterial Biofilms. *Analytical Chemistry* **2014**, *86*, 9139.

(116) Dowlatshahi Pour, M.; Malmberg, P.; Ewing, A. An investigation on the mechanism of sublimed DHB matrix on molecular ion yields in SIMS imaging of brain tissue. *Analytical and Bioanalytical Chemistry* **2016**, *408*, 3071.

(117) Cai, L.; Sheng, L.; Xia, M.; Li, Z.; Zhang, S.; Zhang, X.; Chen, H. Graphene Oxide as a Novel Evenly Continuous Phase Matrix for TOF-SIMS. *Journal of the American Society for Mass Spectrometry* **2017**, *28*, 399.

(118) Škrášková, K.; Claude, E.; Jones, E. A.; Towers, M.; Ellis, S. R.; Heeren, R. M. A. Enhanced capabilities for imaging gangliosides in murine brain with matrix-assisted laser desorption/ionization and desorption electrospray ionization mass spectrometry coupled to ion mobility separation. *Methods* **2016**, *104*, 69.

(119) Eberlin, L. S.; Liu, X.; Ferreira, C. R.; Santagata, S.; Agar, N. Y. R.; Cooks, R. G. Desorption Electrospray Ionization then MALDI Mass Spectrometry Imaging of Lipid and Protein Distributions in Single Tissue Sections. *Analytical Chemistry* **2011**, *83*, 8366.

(120) Prosen, H.; Zupančič-Kralj, L. Solid-phase microextraction. *TrAC Trends in Analytical Chemistry* **1999**, *18*, 272.

(121) Gómez-Ríos, G. A.; Mirabelli, M. F. Solid Phase Microextraction-mass spectrometry: Metanoia. *TrAC Trends in Analytical Chemistry* **2019**, *112*, 201.

(122) Psillakis, E.; Kalogerakis, N. Developments in liquid-phase microextraction. *TrAC Trends in Analytical Chemistry* **2003**, *22*, 565.

(123) Wang, C.-H.; Su, H.; Chou, J.-H.; Lin, J.-Y.; Huang, M.-Z.; Lee, C.-W.; Shiea, J. Multiple solid phase microextraction combined with ambient mass spectrometry for rapid and sensitive detection of trace chemical compounds in aqueous solution. *Analytica Chimica Acta* **2020**, *1107*, 101.

(124) Van Berkel, G. J.; Kertesz, V.; Koepplinger, K. A.; Vavrek, M.; Kong, A.-N. T. Liquid microjunction surface sampling probe electrospray mass spectrometry for detection of drugs and metabolites in thin tissue sections. *Journal of Mass Spectrometry* **2008**, *43*, 500.

(125) Eikel, D.; Vavrek, M.; Smith, S.; Bason, C.; Yeh, S.; Korfsmacher, W. A.; Henion, J. D. Liquid extraction surface analysis mass spectrometry (LESA-MS) as a novel profiling tool for drug distribution and metabolism analysis: the terfenadine example. *Rapid Communications in Mass Spectrometry* **2011**, *25*, 3587.

(126) Cahill, J. F.; Khalid, M.; Retterer, S. T.; Walton, C. L.; Kertesz, V. In Situ Chemical Monitoring and Imaging of Contents within Microfluidic Devices Having a Porous Membrane Wall Using Liquid Microjunction Surface Sampling Probe Mass Spectrometry. *Journal of the American Society for Mass Spectrometry* **2020**, *31*, 832.

(127) Quanico, J.; Franck, J.; Cardon, T.; Leblanc, E.; Wisztorski, M.; Salzet, M.; Fournier, I. NanoLC-MS coupling of liquid microjunction microextraction for on-tissue proteomic analysis. *Biochim Biophys Acta Proteins Proteom* **2017**, *1865*, 891.

(128) May, J. C.; Goodwin, C. R.; Lareau, N. M.; Leaptrot, K. L.; Morris, C. B.; Kurulugama, R. T.; Mordehai, A.; Klein, C.; Barry, W.; Darland, E.; Overney, G.; Imatani, K.; Stafford, G. C.; Fjeldsted, J. C.; McLean, J. A. Conformational Ordering of Biomolecules in the Gas Phase: Nitrogen Collision Cross Sections Measured on a Prototype High Resolution Drift Tube Ion Mobility-Mass Spectrometer. *Analytical Chemistry* **2014**, *86*, 2107.

(129) Valentine, S. J.; Koeniger, S. L.; Clemmer, D. E. A Split-Field Drift Tube for Separation and Efficient Fragmentation of Biomolecular Ions. *Analytical Chemistry* **2003**, *75*, 6202.

(130) Zhong, Y.; Hyung, S.-J.; Ruotolo, B. T. Characterizing the resolution and accuracy of a second-generation traveling-wave ion mobility separator for biomolecular ions. *Analyst* **2011**, *136*, 3534.

(131) Shvartsburg, A. A.; Smith, R. D. Fundamentals of Traveling Wave Ion Mobility Spectrometry. *Analytical Chemistry* **2008**, *80*, 9689.

(132) Purves, R. W.; Guevremont, R. Electrospray Ionization High-Field Asymmetric Waveform Ion Mobility Spectrometry—Mass Spectrometry. *Analytical Chemistry* **1999**, *71*, 2346.

(133) Kolakowski, B. M.; Mester, Z. Review of applications of high-field asymmetric waveform ion mobility spectrometry (FAIMS) and differential mobility spectrometry (DMS). *Analyst* **2007**, *132*, 842.

(134) Guevremont, R. High-field asymmetric waveform ion mobility spectrometry: A new tool for mass spectrometry. *Journal of Chromatography A* **2004**, *1058*, 3.

(135) Fernandez-Lima, F.; Kaplan, D. A.; Suetering, J.; Park, M. A. Gas-phase separation using a trapped ion mobility spectrometer. *International Journal for Ion Mobility Spectrometry* **2011**, *14*, 93.

(136) Michelmann, K.; Silveira, J. A.; Ridgeway, M. E.; Park, M. A. Fundamentals of Trapped Ion Mobility Spectrometry. *Journal of The American Society for Mass Spectrometry* **2015**, *26*, 14.

(137) Groessl, M.; Graf, S.; Knochenmuss, R. High resolution ion mobility-mass spectrometry for separation and identification of isomeric lipids. *Analyst* **2015**, *140*, 6904.

(138) Ridgeway, M. E.; Lubeck, M.; Jordens, J.; Mann, M.; Park, M. A. Trapped ion mobility spectrometry: A short review. *International Journal of Mass Spectrometry* **2018**, *425*, 22.

(139) Fernandez-Lima, F.; Kaplan, D.; Park, M. Note: Integration of trapped ion mobility spectrometry with mass spectrometry. *Review of Scientific Instruments* **2011**, *82*, 126106.

(140) Adams, K. J.; Montero, D.; Aga, D.; Fernandez-Lima, F. Isomer separation of polybrominated diphenyl ether metabolites using nanoESI-TIMS-MS. *International Journal for Ion Mobility Spectrometry* **2016**, *19*, 69.

(141) Ibrahim, Y. M.; Hamid, A. M.; Deng, L.; Garimella, S. V.; Webb, I. K.; Baker, E. S.; Smith, R. D. New frontiers for mass spectrometry based upon structures for lossless ion manipulations. *Analyst* **2017**, *142*, 1010.

(142) Deng, L.; Ibrahim, Y. M.; Baker, E. S.; Aly, N. A.; Hamid, A. M.; Zhang, X.; Zheng, X.; Garimella, S. V. B.; Webb, I. K.; Prost, S. A.; Sandoval, J. A.; Norheim, R. V.; Anderson, G. A.; Tolmachev, A. V.; Smith, R. D. Ion Mobility Separations of Isomers based upon Long Path Length Structures for Lossless Ion Manipulations Combined with Mass Spectrometry. *ChemistrySelect* **2016**, *1*, 2396.

(143) Giles, K.; Ujima, J.; Wildgoose, J.; Pringle, S.; Richardson, K.; Langridge, D.; Green, M. A Cyclic Ion Mobility-Mass Spectrometry System. *Analytical Chemistry* **2019**, *91*, 8564.

(144) Deng, L.; Webb, I. K.; Garimella, S. V.; Hamid, A. M.; Zheng, X.; Norheim, R. V.; Prost, S. A.; Anderson, G. A.; Sandoval, J. A.; Baker, E. S. Serpentine ultralong path with extended routing (SUPER) high resolution traveling wave ion mobility-MS using structures for lossless ion manipulations. *Analytical Chemistry* **2017**, *89*, 4628.

(145) Woods, A. S.; Ugarov, M.; Egan, T.; Koomen, J.; Gillig, K. J.; Fuhrer, K.; Gonin, M.; Schultz, J. A. Lipid/Peptide/Nucleotide Separation with MALDI-Ion Mobility-TOF MS. *Analytical Chemistry* **2004**, *76*, 2187.

(146) McLean, J. A.; Ridenour, W. B.; Caprioli, R. M. Profiling and imaging of tissues by imaging ion mobility-mass spectrometry. *Journal of Mass Spectrometry* **2007**, *42*, 1099.

(147) Spraggins, J. M.; Djambazova, K. V.; Rivera, E. S.; Migas, L. G.; Neumann, E. K.; Fuetterer, A.; Suetering, J.; Goedecke, N.; Ly, A.; Van de Plas, R.; Caprioli, R. M. High-Performance Molecular Imaging with MALDI Trapped Ion-Mobility Time-of-Flight (timsTOF) Mass Spectrometry. *Analytical Chemistry* **2019**, *91*, 14552.

(148) Griffiths, R. L.; Hughes, J. W.; Abbatangelo, S. E.; Belford, M. W.; Styles, I. B.; Cooper, H. J. Comprehensive LESA Mass Spectrometry Imaging of Intact Proteins by Integration of Cylindrical FAIMS. *Analytical Chemistry* **2020**, *92*, 2885.

(149) Klingner, N.; Heller, R.; Hlawacek, G.; Facska, S.; von Borany, J. Time-of-flight secondary ion mass spectrometry in the helium ion microscope. *Ultramicroscopy* **2019**, *198*, 10.

(150) Araki, T. The history of optical microscope. *Mechanical Engineering Reviews* **2017**, *4*, 16.

(151) van Helvoort, T.; Sankaran, N. How Seeing Became Knowing: The Role of the Electron Microscope in Shaping the Modern Definition of Viruses. *Journal of the History of Biology* **2019**, *52*, 125.

(152) Murphy, R. F. Building cell models and simulations from microscope images. *Methods* **2016**, *96*, 33.

(153) Sahl, S. J.; Hell, S. W.; Jakobs, S. Fluorescence nanoscopy in cell biology. *Nature Reviews Molecular Cell Biology* **2017**, *18*, 685.

(154) Kumarasinghe, M. P.; Bourke, M. J.; Brown, I.; Draganov, P. V.; McLeod, D.; Streutker, C.; Raftopoulos, S.; Ushiku, T.; Lauwers, G. Y. Pathological assessment of endoscopic resections of the gastrointestinal tract: a comprehensive clinicopathologic review. *Modern Pathology* **2020**.

(155) Deschaine, M. A.; Lehman, J. S. The interface reaction pattern in the skin: an integrated review of clinical and pathological features. *Human Pathology* **2019**, *91*, 86.

(156) Picard, C.; Orbach, D.; Carton, M.; Brugieres, L.; Renaudin, K.; Aubert, S.; Berrebi, D.; Galmiche, L.; Dujardin, F.; Leblond, P.; Thomas-Teinturier, C.; Dijoud, F. Revisiting the role of the pathological grading in pediatric adrenal cortical tumors: results from a national cohort study with pathological review. *Modern Pathology* **2019**, *32*, 546.

(157) Sun, C.; Liu, W.; Mu, Y.; Wang, X. 1,1'-binaphthyl-2,2'-diamine as a novel MALDI matrix to enhance the *in situ* imaging of metabolic heterogeneity in lung cancer. *Talanta* **2020**, *209*, 120557.

(158) Wang, Y.; Hinz, S.; Uckermann, O.; Hönscheid, P.; von Schönfels, W.; Burmeister, G.; Hendricks, A.; Ackerman, J. M.; Baretton, G. B.; Hampe, J.; Brosch, M.; Schafmayer, C.; Shevchenko, A.; Zeissig, S. Shotgun lipidomics-based characterization of the landscape of lipid metabolism in colorectal cancer. *Biochimica et Biophysica Acta (BBA) - Molecular and Cell Biology of Lipids* **2020**, *1865*, 158579.

(159) Andersen, M. K.; Krossa, S.; Høiem, T. S.; Buchholz, R.; Claes, B. S. R.; Balluff, B.; Ellis, S. R.; Richardsen, E.; Bertilsson, H.; Heeren, R. M. A.; Bathen, T. F.; Karst, U.; Giskeødegård, G. F.; Tessem, M.-B. Simultaneous Detection of Zinc and Its Pathway Metabolites Using MALDI MS Imaging of Prostate Tissue. *Analytical Chemistry* **2020**, *92*, 3171.

(160) Marsilio, S.; Newman, S. J.; Estep, J. S.; Giarettta, P. R.; Lidbury, J. A.; Warry, E.; Flory, A.; Morley, P. S.; Smoot, K.; Seeley, E. H.; Powell, M. J.; Suchodolski, J. S.; Steiner, J. M. Differentiation of lymphocytic-plasmacytic enteropathy and small cell lymphoma in cats using histology-guided mass spectrometry. *Journal of Veterinary Internal Medicine* **2020**, *34*, 669.

(161) Cordeiro, F. B.; Jarmusch, A. K.; León, M.; Ferreira, C. R.; Pirro, V.; Eberlin, L. S.; Hallett, J.; Miglino, M. A.; Cooks, R. G. Mammalian ovarian lipid distributions by desorption electrospray ionization-mass spectrometry (DESI-MS) imaging. *Analytical and Bioanalytical Chemistry* **2020**, *412*, 1251.

(162) Zhang, G.; Zhang, J.; DeHoog, R. J.; Pennathur, S.; Anderton, C. R.; Venkatachalam, M. A.; Alexandrov, T.; Eberlin, L. S.; Sharma, K. DESI-MSI and METASPACE indicates lipid abnormalities and altered mitochondrial membrane components in diabetic renal proximal tubules. *Metabolomics* **2020**, *16*, 11.

(163) Severiano, D. L. R.; Oliveira-Lima, O. C.; Vasconcelos, G. A.; Lemes Marques, B.; Almeida de Carvalho, G.; Freitas, E. M. M.; Xavier, C. H.; Gomez, M. V.; Pinheiro, A. C. O.; Gomez, R. S.; Vaz, B. G.; Pinto, M. C. X. Cerebral Lipid Dynamics in Chronic Cerebral Hypoperfusion Model by DESI-MS Imaging. *Neuroscience* **2020**, *426*, 1.

(164) Basu, S. S.; Regan, M. S.; Randall, E. C.; Abdelmoula, W. M.; Clark, A. R.; Gimenez-Cassina Lopez, B.; Cornett, D. S.; Haase, A.; Santagata, S.; Agar, N. Y. R. Rapid MALDI mass spectrometry imaging for surgical pathology. *npj Precision Oncology* **2019**, *3*, 17.

(165) Sun, C.; Zhang, M.; Dong, H.; Liu, W.; Guo, L.; Wang, X. A spatially-resolved approach to visualize the distribution and biosynthesis of flavones in *Scutellaria baicalensis* Georgi. *Journal of Pharmaceutical and Biomedical Analysis* **2020**, *179*, 113014.

(166) Sun, C.; Liu, W.; Ma, S.; Zhang, M.; Geng, Y.; Wang, X. Development of a high-coverage matrix-assisted laser desorption/ionization mass spectrometry imaging method for visualizing the spatial dynamics of functional metabolites in *Salvia miltiorrhiza* Bge. *Journal of Chromatography A* **2020**, *1614*, 460704.

(167) Patterson, N. H.; Tuck, M.; Lewis, A.; Kaushansky, A.; Norris, J. L.; Van de Plas, R.; Caprioli, R. M. Next Generation Histology-Directed Imaging Mass Spectrometry Driven by Autofluorescence Microscopy. *Analytical Chemistry* **2018**, *90*, 12404.

(168) Patterson, N. H.; Tuck, M.; Van de Plas, R.; Caprioli, R. M. Advanced Registration and Analysis of MALDI Imaging Mass Spectrometry Measurements through Autofluorescence Microscopy. *Analytical Chemistry* **2018**, *90*, 12395.

(169) Goltsev, Y.; Samusik, N.; Kennedy-Darling, J.; Bhate, S.; Hale, M.; Vazquez, G.; Black, S.; Nolan, G. P. Deep Profiling of Mouse Splenic Architecture with CODEX Multiplexed Imaging. *Cell* **2018**, *174*, 968.

(170) Eng, J.; Thibault, G.; Luoh, S.-W.; Gray, J. W.; Chang, Y. H.; Chin, K. In *Biomarkers for Immunotherapy of Cancer*:

Methods and Protocols; Thurin, M., Cesano, A., Marincola, F. M., Eds.; Springer New York: New York, NY, 2020, p 521.

(171) Rashid, R.; Gaglia, G.; Chen, Y.-A.; Lin, J.-R.; Du, Z.; Maliga, Z.; Schapiro, D.; Yapp, C.; Muhlich, J.; Sokolov, A.; Sorger, P.; Santagata, S. Highly multiplexed immunofluorescence images and single-cell data of immune markers in tonsil and lung cancer. *Scientific Data* **2019**, *6*, 323.

(172) Lin, T.; Jin, H.; Gong, L.; Yu, R.; Sun, S.; Yang, L.; Zhang, P.; Han, P.; Cheng, J.; Liu, L.; Wei, Q. Surveillance of non-muscle invasive bladder cancer using fluorescence *in situ* hybridization: Protocol for a systematic review and meta-analysis. *Medicine (Baltimore)* **2019**, *98*, e14573.

(173) Miedema, J.; Andea, A. A. Through the looking glass and what you find there: making sense of comparative genomic hybridization and fluorescence *in situ* hybridization for melanoma diagnosis. *Modern Pathology* **2020**.

(174) Schleyer, G.; Shahaf, N.; Ziv, C.; Dong, Y.; Meoded, R. A.; Helfrich, E. J. N.; Schatz, D.; Rosenwasser, S.; Rogachev, I.; Aharoni, A.; Piel, J.; Vardi, A. In plaque-mass spectrometry imaging of a bloom-forming alga during viral infection reveals a metabolic shift towards odd-chain fatty acid lipids. *Nature Microbiology* **2019**, *4*, 527.

(175) Solier, C.; Langen, H. Antibody-based proteomics and biomarker research—Current status and limitations. *PROTEOMICS* **2014**, *14*, 774.

(176) Budnik, B.; Levy, E.; Harmange, G.; Slavov, N. SCoPE-MS: mass spectrometry of single mammalian cells quantifies proteome heterogeneity during cell differentiation. *Genome Biology* **2018**, *19*, 161.

(177) Kriegsmann, K.; Longuespée, R.; Hundemer, M.; Zgorzelski, C.; Casadonte, R.; Schwamborn, K.; Weichert, W.; Schirmacher, P.; Harms, A.; Kazdal, D.; Leichsenring, J.; Stenzinger, A.; Warth, A.; Fresnais, M.; Kriegsmann, J.; Kriegsmann, M. Combined Immunohistochemistry after Mass Spectrometry Imaging for Superior Spatial Information. *PROTEOMICS – Clinical Applications* **2019**, *13*, 1800035.

(178) Kaya, I.; Michno, W.; Brinet, D.; Iacone, Y.; Zanni, G.; Blennow, K.; Zetterberg, H.; Hanrieder, J. Histology-Compatible MALDI Mass Spectrometry Based Imaging of Neuronal Lipids for Subsequent Immunofluorescent Staining. *Analytical Chemistry* **2017**, *89*, 4685.

(179) Tominski, C.; Lösekann-Behrens, T.; Ruecker, A.; Hagemann, N.; Kleindienst, S.; Mueller, C. W.; Höschen, C.; Kögel-Knabner, I.; Kappler, A.; Behrens, S. Insights into Carbon Metabolism Provided by Fluorescence *In Situ* Hybridization-Secondary Ion Mass Spectrometry Imaging of an Autotrophic, Nitrate-Reducing, Fe(II)-Oxidizing Enrichment Culture. *Applied and Environmental Microbiology* **2018**, *84*, e02166.

(180) Huber, K.; Kunzke, T.; Buck, A.; Langer, R.; Luber, B.; Feuchtinger, A.; Walch, A. Multimodal analysis of formalin-fixed and paraffin-embedded tissue by MALDI imaging and fluorescence *in situ* hybridization for combined genetic and metabolic analysis. *Laboratory Investigation* **2019**, *99*, 1535.

(181) Dekas, A. E.; Orphan, V. J. In *Methods in Enzymology*; Klotz, M. G., Ed.; Academic Press: 2011; Vol. 486, p 281.

(182) Jones, M. A.; Cho, S. H.; Patterson, N. H.; Van de Plas, R.; Spraggins, J. M.; Boothby, M. R.; Caprioli, R. M. Discovering New Lipidomic Features Using Cell Type Specific Fluorophore Expression to Provide Spatial and Biological Specificity in a Multimodal Workflow with MALDI Imaging Mass Spectrometry. *Analytical Chemistry* **2020**, *92*, 7079.

(183) Vanickova, L.; Guran, R.; Kollar, S.; Emri, G.; Krizkova, S.; Do, T.; Heger, Z.; Zitka, O.; Adam, V. Mass spectrometric imaging of cysteine rich proteins in human skin. *International Journal of Biological Macromolecules* **2019**, *125*, 270.

(184) Zhang, Z.; Sugiura, Y.; Mune, T.; Nishiyama, M.; Terada, Y.; Mukai, K.; Nishimoto, K. Immunohistochemistry for aldosterone synthase CYP11B2 and matrix-assisted laser desorption ionization imaging mass spectrometry for *in-situ* aldosterone detection. *Current Opinion in Nephrology and Hypertension* **2019**, *28*, 105.

(185) Prentice, B. M.; Hart, N. J.; Phillips, N.; Haliyur, R.; Judd, A.; Armandala, R.; Spraggins, J. M.; Lowe, C. L.; Boyd, K. L.; Stein, R. W.; Wright, C. V.; Norris, J. L.; Powers, A. C.; Brissova, M.; Caprioli, R. M. Imaging mass spectrometry enables molecular profiling of mouse and human pancreatic tissue. *Diabetologia* **2019**, *62*, 1036.

(186) Bien, T.; Perl, M.; Machmüller, A. C.; Nitsche, U.; Conrad, A.; Johannes, L.; Müthing, J.; Soltwisch, J.; Janssen, K.-P.; Dreisewerd, K. MALDI-2 Mass Spectrometry and Immunohistochemistry Imaging of Gb3Cer, Gb4Cer, and Further Glycosphingolipids in Human Colorectal Cancer Tissue. *Analytical Chemistry* **2020**, *92*, 7096.

(187) Prade, V. M.; Kunzke, T.; Feuchtinger, A.; Rohm, M.; Luber, B.; Lordick, F.; Buck, A.; Walch, A. De novo discovery of metabolic heterogeneity with immunophenotype-guided imaging mass spectrometry. *Molecular Metabolism* **2020**, *36*, 100953.

(188) Rabe, J.-H.; A. Sammour, D.; Schulz, S.; Munteanu, B.; Ott, M.; Ochs, K.; Hohenberger, P.; Marx, A.; Platten, M.; Opitz, C. A.; Ory, D. S.; Hopf, C. Fourier Transform Infrared Microscopy Enables Guidance of Automated Mass Spectrometry Imaging to Predefined Tissue Morphologies. *Scientific Reports* **2018**, *8*, 313.

(189) Jiang, H.; Kilburn, M. R.; Decelle, J.; Musat, N. NanoSIMS chemical imaging combined with correlative microscopy for biological sample analysis. *Current Opinion in Biotechnology* **2016**, *41*, 130.

(190) Lovrić, J.; Dunevall, J.; Larsson, A.; Ren, L.; Andersson, S.; Meibom, A.; Malmberg, P.; Kuczy, M. E.; Ewing, A. G. Nano Secondary Ion Mass Spectrometry Imaging of Dopamine Distribution Across Nanometer Vesicles. *ACS Nano* **2017**, *11*, 3446.

(191) Liu, W.; Huang, L.; Komorek, R.; Handakumbura, P.; Zhou, Y.; Hu, D.; Engelhard, M. H.; Jiang, H.; Yu, X.-Y.; Jansson, C.; Zhu, Z. Correlative surface imaging reveals chemical signatures for bacterial hotspots on plant roots. *Analyst* **2020**, *145*, 393.

(192) Strnad, Š.; Praženková, V.; Sýkora, D.; Cvačka, J.; Maletinská, L.; Popelová, A.; Vrkoslav, V. The use of 1,5-diaminonaphthalene for matrix-assisted laser desorption/ionization mass spectrometry imaging of brain in neurodegenerative disorders. *Talanta* **2019**, *201*, 364.

(193) Yang, H.; Su, R.; Wishnok, J. S.; Liu, N.; Chen, C.; Liu, S.; Tannenbaum, S. R. Magnetic silica nanoparticles for use in matrix-assisted laser desorption ionization mass spectrometry of labile biomolecules such as oligosaccharides, amino acids, peptides and nucleosides. *Microchimica Acta* **2019**, *186*, 104.

(194) Baker, M. J.; Trevisan, J.; Bassan, P.; Bhargava, R.; Butler, H. J.; Dorling, K. M.; Fielden, P. R.; Fogarty, S. W.; Fullwood, N. J.; Heys, K. A.; Hughes, C.; Lasch, P.; Martin-Hirsch, P. L.; Obinaju, B.; Sockalingum, G. D.; Sulé-Suso, J.; Strong, R. J.; Walsh, M. J.; Wood, B. R.; Gardner, P.; Martin, F. L. Using Fourier transform IR spectroscopy to analyze biological materials. *Nature Protocols* **2014**, *9*, 1771.

(195) Masyuko, R.; Lanni, E. J.; Sweedler, J. V.; Bohn, P. W. Correlated imaging – a grand challenge in chemical analysis. *Analyst* **2013**, *138*, 1924.

(196) Rinia, H. A.; Burger, K. N. J.; Bonn, M.; Müller, M. Quantitative Label-Free Imaging of Lipid Composition and Packing of Individual Cellular Lipid Droplets Using Multiplex CARS Microscopy. *Biophysical journal* **2008**, *95*, 4908.

(197) Le, T. T.; Duren, H. M.; Slipchenko, M. N.; Hu, C.-D.; Cheng, J.-X. Label-free quantitative analysis of lipid metabolism in living Caenorhabditis elegans. *Journal of Lipid Research* **2010**, *51*, 672.

(198) Li, J.; Condello, S.; Thomas-Pepin, J.; Ma, X.; Xia, Y.; Hurley, T. D.; Matei, D.; Cheng, J.-X. Lipid Desaturation Is a Metabolic Marker and Therapeutic Target of Ovarian Cancer Stem Cells. *Cell Stem Cell* **2017**, *20*, 303.

(199) Tipping, W. J.; Lee, M.; Serrels, A.; Brunton, V. G.; Hulme, A. N. Stimulated Raman scattering microscopy: an emerging tool for drug discovery. *Chemical Society Reviews* **2016**, *45*, 2075.

(200) Meister, K.; Niesel, J.; Schatzschneider, U.; Metzler-Nolte, N.; Schmidt, D. A.; Haverin, M. Label-Free Imaging of Metal-Carbonyl Complexes in Live Cells by Raman Microspectroscopy. *Angewandte Chemie International Edition* **2010**, *49*, 3310.

(201) Yamakoshi, H.; Dodo, K.; Palonpon, A.; Ando, J.; Fujita, K.; Kawata, S.; Sodeoka, M. Alkyne-Tag Raman Imaging for Visualization of Mobile Small Molecules in Live Cells. *Journal of the American Chemical Society* **2012**, *134*, 20681.

(202) Lazaro-Pacheco, D.; Shaaban, A. M.; Rehman, S.; Rehman, I. Raman spectroscopy of breast cancer. *Applied Spectroscopy Reviews* **2019**, *1*.

(203) Ralbovsky, N. M.; Lednev, I. K. Raman spectroscopy and chemometrics: A potential universal method for diagnosing cancer. *Spectrochimica Acta Part A: Molecular and Biomolecular Spectroscopy* **2019**, *219*, 463.

(204) Wiercigroch, E.; Szafraniec, E.; Czamara, K.; Pacia, M. Z.; Majzner, K.; Kochan, K.; Kaczor, A.; Baranska, M.; Malek, K. Raman and infrared spectroscopy of carbohydrates: A review. *Spectrochimica Acta Part A: Molecular and Biomolecular Spectroscopy* **2017**, *185*, 317.

(205) Gautam, R.; Vanga, S.; Ariese, F.; Umapathy, S. Review of multidimensional data processing approaches for Raman and infrared spectroscopy. *EPJ Techniques and Instrumentation* **2015**, *2*, 8.

(206) Lasch, P.; Noda, I. Two-Dimensional Correlation Spectroscopy for Multimodal Analysis of FT-IR, Raman, and MALDI-TOF MS Hyperspectral Images with Hamster Brain Tissue. *Analytical Chemistry* **2017**, *89*, 5008.

(207) Tai, T.; Karácsony, O.; Bocharova, V.; Van Berkel, G. J.; Kertesz, V. Topographical and Chemical Imaging of a Phase Separated Polymer Using a Combined Atomic Force Microscopy/Infrared Spectroscopy/Mass Spectrometry Platform. *Analytical Chemistry* **2016**, *88*, 2864.

(208) Balbekova, A.; Lohninger, H.; van Tilborg, G. A. F.; Dijkhuizen, R. M.; Bonta, M.; Limbeck, A.; Lendl, B.; Al-Saad, K. A.; Ali, M.; Celikic, M.; Ofner, J. Fourier Transform Infrared (FT-IR) and Laser Ablation Inductively Coupled Plasma–Mass Spectrometry (LA-ICP-MS) Imaging of Cerebral Ischemia: Combined Analysis of Rat Brain Thin Cuts Toward Improved Tissue Classification. *Applied Spectroscopy* **2018**, *72*, 241.

(209) Neumann, E. K.; Comi, T. J.; Spegazzini, N.; Mitchell, J. W.; Rubakhin, S. S.; Gillette, M. U.; Bhargava, R.; Sweedler, J. V. Multimodal Chemical Analysis of the Brain by High Mass Resolution Mass Spectrometry and Infrared Spectroscopic Imaging. *Analytical Chemistry* **2018**, *90*, 11572.

(210) Chisanga, M.; Linton, D.; Muhamadali, H.; Ellis, D. I.; Kimber, R. L.; Mironov, A.; Goodacre, R. Rapid differentiation of *Campylobacter jejuni* cell wall mutants using Raman spectroscopy, SERS and mass spectrometry combined with chemometrics. *Analyst* **2020**, *145*, 1236.

(211) Dunham, S. J. B.; Ellis, J. F.; Baig, N. F.; Morales-Soto, N.; Cao, T.; Shrout, J. D.; Bohn, P. W.; Sweedler, J. V. Quantitative SIMS Imaging of Agar-Based Microbial Communities. *Analytical Chemistry* **2018**, *90*, 5654.

(212) Morales-Soto, N.; Dunham, S. J. B.; Baig, N. F.; Ellis, J. F.; Madukoma, C. S.; Bohn, P. W.; Sweedler, J. V.; Shrout, J. D. Spatially dependent alkyl quinolone signaling responses to antibiotics in *Pseudomonas aeruginosa* swarms. *Journal of Biological Chemistry* **2018**, *293*, 9544.

(213) Burkhow, S. J.; Stephens, N. M.; Mei, Y.; Dueñas, M. E.; Freppon, D. J.; Ding, G.; Smith, S. C.; Lee, Y.-J.; Nikolau, B. J.; Whitham, S. A.; Smith, E. A. Characterizing virus-induced gene silencing at the cellular level with *in situ* multimodal imaging. *Plant Methods* **2018**, *14*, 37.

(214) Ali, A.; Abouleila, Y.; Shimizu, Y.; Hiyama, E.; Watanabe, T. M.; Yanagida, T.; Germond, A. Single-Cell Screening of Tamoxifen Abundance and Effect Using Mass Spectrometry and Raman-Spectroscopy. *Analytical Chemistry* **2019**, *91*, 2710.

(215) Ryabchikov, O.; Popp, J.; Bocklitz, T. Fusion of MALDI Spectrometric Imaging and Raman Spectroscopic Data for the Analysis of Biological Samples. *Frontiers in Chemistry* **2018**, *6*.

(216) Bergholt, M. S.; Serio, A.; McKenzie, J. S.; Boyd, A.; Soares, R. F.; Tillner, J.; Chiappini, C.; Wu, V.; Dannhorn, A.; Takats, Z.; Williams, A.; Stevens, M. M. Correlated Heterospectral Lipidomics for Biomolecular Profiling of Remyelination in Multiple Sclerosis. *ACS Central Science* **2018**, *4*, 39.

(217) Bakry, R.; Rainer, M.; Huck, C. W.; Bonn, G. K. Protein profiling for cancer biomarker discovery using matrix-assisted laser desorption/ionization time-of-flight mass spectrometry and infrared imaging: A review. *Analytica Chimica Acta* **2011**, *690*, 26.

(218) Petit, V. W.; Réfrégiers, M.; Guettier, C.; Jamme, F.; Sebanayakam, K.; Brunelle, A.; Laprévote, O.; Dumas, P.; Le Naour, F. Multimodal Spectroscopy Combining Time-of-Flight-Secondary Ion Mass Spectrometry, Synchrotron-FT-IR, and Synchrotron-UV

Microspectroscopies on the Same Tissue Section. *Analytical Chemistry* **2010**, *82*, 3963.

(219) Lohöfer, F.; Hoffmann, L.; Buchholz, R.; Huber, K.; Glinzer, A.; Kosanke, K.; Feuchtinger, A.; Aichler, M.; Feuerecker, B.; Kaassis, G.; Rummery, E. J.; Höltke, C.; Faber, C.; Schilling, F.; Botnar, R. M.; Walch, A. K.; Karst, U.; Wildgruber, M. Molecular imaging of myocardial infarction with Gadofluorine P – A combined magnetic resonance and mass spectrometry imaging approach. *Heliyon* **2018**, *4*, e00606.

(220) Lohöfer, F.; Buchholz, R.; Glinzer, A.; Huber, K.; Haas, H.; Kaassis, G.; Feuchtinger, A.; Aichler, M.; Sporns, P. B.; Höltke, C.; Stölting, M.; Schilling, F.; Botnar, R. M.; Kimm, M. A.; Faber, C.; Walch, A. K.; Zernecke, A.; Karst, U.; Wildgruber, M. Mass Spectrometry Imaging of atherosclerosis-affine Gadofluorine following Magnetic Resonance Imaging. *Scientific Reports* **2020**, *10*, 79.

(221) Srimany, A.; George, C.; Naik, H. R.; Pinto, D. G.; Chandrakumar, N.; Pradeep, T. Developmental patterning and segregation of alkaloids in areca nut (seed of Areca catechu) revealed by magnetic resonance and mass spectrometry imaging. *Phytochemistry* **2016**, *125*, 35.

(222) Verbeeck, N.; Spraggins, J. M.; Murphy, M. J. M.; Wang, H.-d.; Deutch, A. Y.; Caprioli, R. M.; Van de Plas, R. Connecting imaging mass spectrometry and magnetic resonance imaging-based anatomical atlases for automated anatomical interpretation and differential analysis. *Biochimica et Biophysica Acta (BBA) - Proteins and Proteomics* **2017**, *1865*, 967.

(223) Marshall, D. D.; Powers, R. Beyond the paradigm: Combining mass spectrometry and nuclear magnetic resonance for metabolomics. *Progress in Nuclear Magnetic Resonance Spectroscopy* **2017**, *100*, 1.

(224) Cassat, J. E.; Moore, J. L.; Wilson, K. J.; Stark, Z.; Prentice, B. M.; Van de Plas, R.; Perry, W. J.; Zhang, Y.; Virostko, J.; Colvin, D. C.; Rose, K. L.; Judd, A. M.; Reyzer, M. L.; Spraggins, J. M.; Grunenwald, C. M.; Gore, J. C.; Caprioli, R. M.; Skaar, E. P. Integrated molecular imaging reveals tissue heterogeneity driving host-pathogen interactions. *Science Translational Medicine* **2018**, *10*, eaan6361.

(225) Wang, Z.; Gerstein, M.; Snyder, M. RNA-Seq: a revolutionary tool for transcriptomics. *Nature Reviews Genetics* **2009**, *10*, 57.

(226) Horgan, R. P.; Kenny, L. C. ‘Omic’ technologies: genomics, transcriptomics, proteomics and metabolomics. *The Obstetrician & Gynaecologist* **2011**, *13*, 189.

(227) Kulkarni, A.; Anderson, A. G.; Merullo, D. P.; Konopka, G. Beyond bulk: a review of single cell transcriptomics methodologies and applications. *Current Opinion in Biotechnology* **2019**, *58*, 129.

(228) Wang, Z.; Shi, H.; Yu, S.; Zhou, W.; Li, J.; Liu, S.; Deng, M.; Ma, J.; Wei, Y.; Zheng, Y.; Liu, Y. Comprehensive transcriptomics, proteomics, and metabolomics analyses of the mechanisms regulating tiller production in low-tillering wheat. *Theoretical and Applied Genetics* **2019**, *132*, 2181.

(229) Angelidis, I.; Simon, L. M.; Fernandez, I. E.; Strunz, M.; Mayr, C. H.; Greiffo, F. R.; Tsitsirisidis, G.; Ansari, M.; Graf, E.; Strom, T.-M.; Nagendran, M.; Desai, T.; Eickelberg, O.; Mann, M.; Theis, F. J.; Schiller, H. B. An atlas of the aging lung mapped by single cell transcriptomics and deep tissue proteomics. *Nature Communications* **2019**, *10*, 963.

(230) Liessem, S.; Ragionieri, L.; Neupert, S.; Büschges, A.; Predel, R. Transcriptomic and Neuropeptidomic Analysis of the Stick Insect, *Carausius morosus*. *Journal of Proteome Research* **2018**, *17*, 2192.

(231) Sung, C.-C.; Chen, L.; Limbutara, K.; Jung, H. J.; Gilmer, G. G.; Yang, C.-R.; Lin, S.-H.; Khositseth, S.; Chou, C.-L.; Knepper, M. A. RNA-Seq and protein mass spectrometry in microdissected kidney tubules reveal signaling processes initiating lithium-induced nephrogenic diabetes insipidus. *Kidney International* **2019**, *96*, 363.

(232) Noble, K. V.; Reyzer, M. L.; Barth, J. L.; McDonald, H.; Tuck, M.; Schey, K. L.; Krug, E. L.; Lang, H. Use of Proteomic Imaging Coupled With Transcriptomic Analysis to Identify Biomolecules Responsive to Cochlear Injury. *Frontiers in Molecular Neuroscience* **2018**, *11*.

(233) Kawashima, M.; Tokiwa, M.; Nishimura, T.; Kawata, Y.; Sugimoto, M.; Kataoka, T. R.; Sakurai, T.; Iwaisako, K.; Suzuki, E.; Hagiwara, M.; Harris, A. L.; Toi, M. High-resolution imaging mass spectrometry combined with transcriptomic analysis identified a link

1 between fatty acid composition of phosphatidylinositols and the immune
2 checkpoint pathway at the primary tumour site of breast cancer. *British*
3 *Journal of Cancer* **2020**, *122*, 245.

4 (234) Jarvis, S.; Gethings, L.; Gadeleta, R.; Claude, E.;
5 Winston, R.; Williamson, C.; Bevan, C. In *Society for Endocrinology BES*
6 2018; BioScientifica: 2018; Vol. 59.

7 (235) Dunevall, J.; Majdi, S.; Larsson, A.; Ewing, A.
8 Vesicle impact electrochemical cytometry compared to amperometric
9 exocytosis measurements. *Current Opinion in Electrochemistry* **2017**, *5*,
10 85.

11 (236) Chen, C.-C.; Cang, C.; Fenske, S.; Butz, E.; Chao,
12 Y.-K.; Biel, M.; Ren, D.; Wahl-Schott, C.; Grimm, C. Patch-clamp
13 technique to characterize ion channels in enlarged individual
14 endolysosomes. *Nature Protocols* **2017**, *12*, 1639.

15 (237) Leyrer-Jackson, J. M.; Olive, M. F.; Gipson, C. D. In
16 *Glutamate Receptors: Methods and Protocols*; Burger, C., Velardo, M. J.,
17 Eds.; Springer New York: New York, NY, 2019, p 107.

18 (238) Phan, N. T. N.; Li, X.; Ewing, A. G. Measuring
19 synaptic vesicles using cellular electrochemistry and nanoscale molecular
20 imaging. *Nature Reviews Chemistry* **2017**, *1*, 0048.

21 (239) Li, K.; Liu, J.; Grovenor, C. R. M.; Moore, K. L.
22 NanoSIMS Imaging and Analysis in Materials Science. *Annual Review of
23 Analytical Chemistry* **2020**, *13*, null.

24 (240) Ranjbari, E.; Majdi, S.; Ewing, A. Analytical
25 Techniques: Shedding Light upon Nanometer-Sized Secretory Vesicles.
26 *Trends in Chemistry* **2019**, *1*, 440.

27 (241) Chadwick, G. L.; Jiménez Otero, F.; Gralnick, J. A.;
28 Bond, D. R.; Orphan, V. J. NanoSIMS imaging reveals metabolic
29 stratification within current-producing biofilms. *Proceedings of the
30 National Academy of Sciences* **2019**, *116*, 20716.

31 (242) Thomen, A.; Najafinobar, N.; Penen, F.; Kay, E.;
32 Upadhyay, P. P.; Li, X.; Phan, N. T. N.; Malmberg, P.; Klarqvist, M.;
33 Andersson, S.; Kurczy, M. E.; Ewing, A. G. Subcellular Mass Spectrometry
34 Imaging and Absolute Quantitative Analysis across Organelles. *ACS Nano*
35 **2020**.

36 (243) Larsson, A.; Majdi, S.; Oleinick, A.; Svir, I.;
37 Dunevall, J.; Amatore, C.; Ewing, A. G. Intracellular Electrochemical
38 Nanomeasurements Reveal that Exocytosis of Molecules at Living Neurons
39 is Subquantal and Complex. *Angewandte Chemie International Edition*
40 **2020**, *59*, 6711.

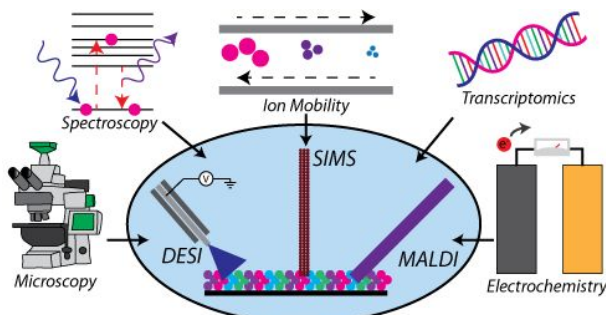
41 (244) Baker, L. A.; Jagdale, G. S. On the intersection of
42 electrochemistry and mass spectrometry. *Current Opinion in
43 Electrochemistry* **2019**, *13*, 140.

44 (245) Lin, L.-E.; Chen, C.-L.; Huang, Y.-C.; Chung, H.-H.;
45 Lin, C.-W.; Chen, K.-C.; Peng, Y.-J.; Ding, S.-T.; Wang, M.-Y.; Shen, T.-
46 L.; Hsu, C.-C. Precision biomarker discovery powered by microscopy
47 image fusion-assisted high spatial resolution ambient ionization mass
spectrometry imaging. *Analytica Chimica Acta* **2020**, *1100*, 75.

48 (246) Van de Plas, R.; Yang, J.; Spraggins, J.; Caprioli, R.
49 M. Image fusion of mass spectrometry and microscopy: a multimodality
50 paradigm for molecular tissue mapping. *Nature Methods* **2015**, *12*, 366.

51 (247) Lin, L.-E.; Chen, C.-L.; Huang, Y.-C.; Chung, H.-H.;
52 Lin, C.-W.; Chen, K.-C.; Peng, Y.-J.; Ding, S.-T.; Wang, M.-Y.; Shen, T.-
53 L.; Hsu, C.-C. High Spatial Resolution Ambient Ionization Mass
54 Spectrometry Imaging Using Microscopy Image Fusion Determines Tumor
55 Margins. *bioRxiv* **2019**, 657494.

56 (248) Vollnhals, F.; Audinot, J.-N.; Wirtz, T.; Mercier-
57 Bonin, M.; Fourquaux, I.; Schroepel, B.; Kraushaar, U.; Lev-Ram, V.;
58 Ellisman, M. H.; Eswara, S. Correlative Microscopy Combining Secondary
59 Ion Mass Spectrometry and Electron Microscopy: Comparison of Intensity-
60 Hue-Saturation and Laplacian Pyramid Methods for Image Fusion.
Analytical Chemistry **2017**, *89*, 10702.



TOC Graphic

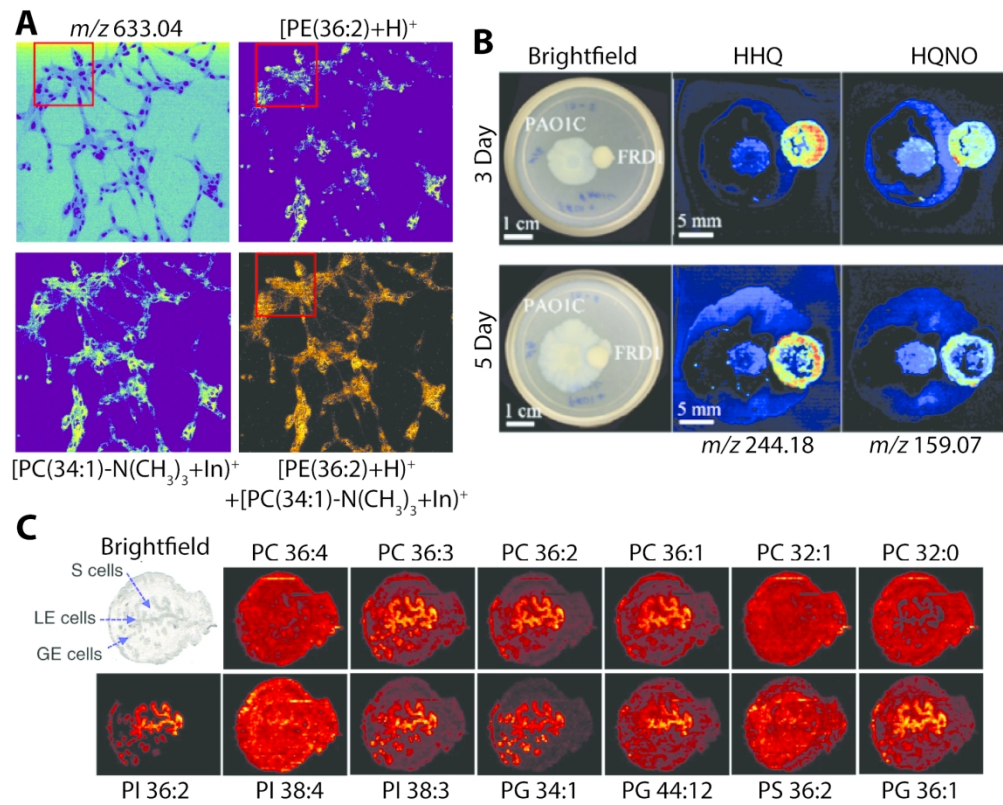


Figure 1. Selected developments within the IMS community. Image of a Vero B cell culture at 1 μ m spatial resolution acquired with transition mode MALDI-2 IMS developed by the Dreiswerd lab (A). Panel A is adapted with permission from ref47, Niehaus, M. et al. *Nat Methods* 16, 925–931 (2019). Copyright 2019 Nature Publishing. SIMS image of a coculture of different *Pseudomonas aeruginosa* stains visualized with different signaling small molecules (B). Panel B is adapted with permission from ref24,48, Cao, T. et al. *SPIE BiOS* 108630A (2019). Copyright 2019 SPIE. Digital Library. Lipid images both positive and negative mode of the human eye using nanoDESI at 10 μ m spatial resolution (C). Panel C is adapted with permission from ref49–51, Yin, R. et al. *Nature Protocols* 14, 3445–3470 (2019). Copyright 2019 Nature Publishing.

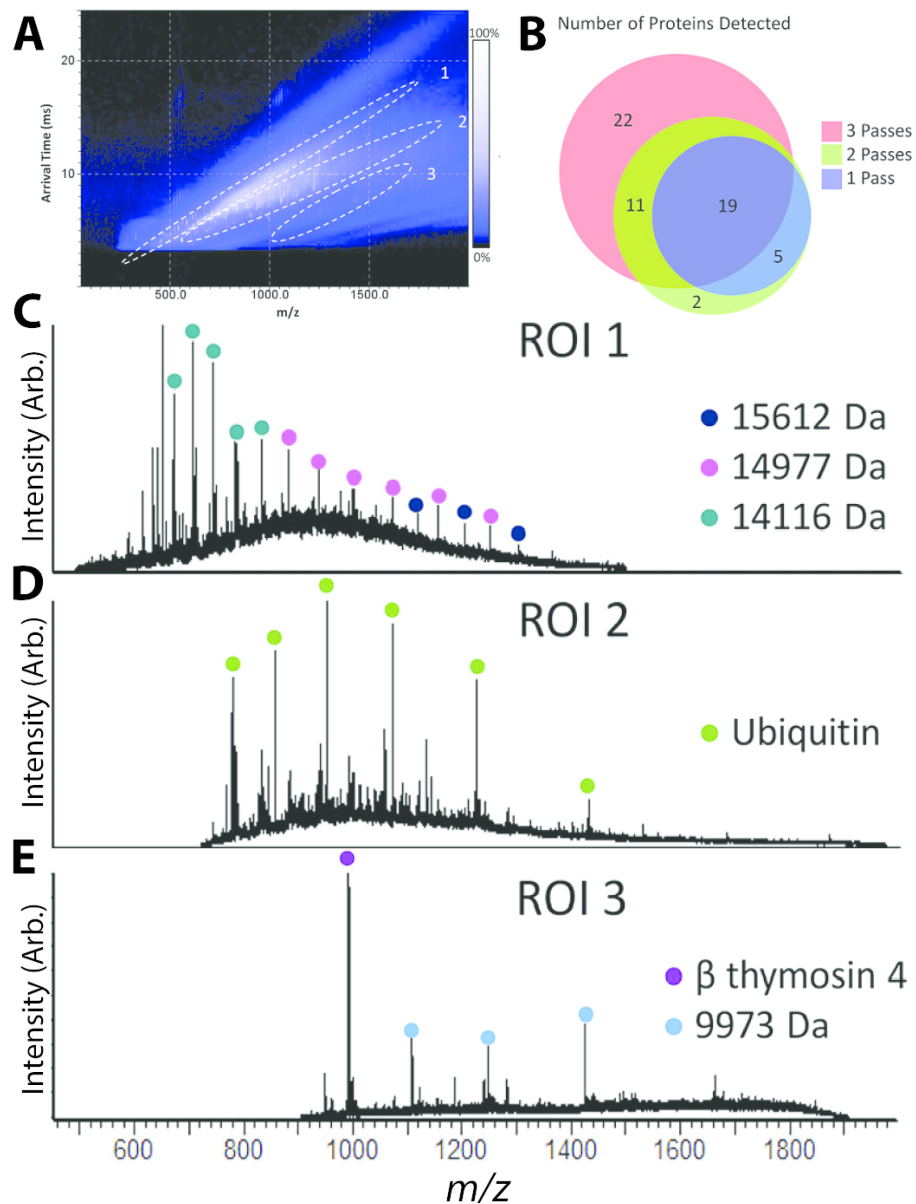


Figure 2. LESA and cIM analysis of a complex murine kidney protein extract. More proteins are detected after each additional cycle of cIM (A). IM heat map generated from a single cycle of cIM (B), where extracted mass spectra from different trend lines contain different protein signatures (C-E). This figure is adapted with permission from ref109, Sisley, E.K. et al. Analytical Chemistry (2020). Copyright 2020 American Chemical Society.

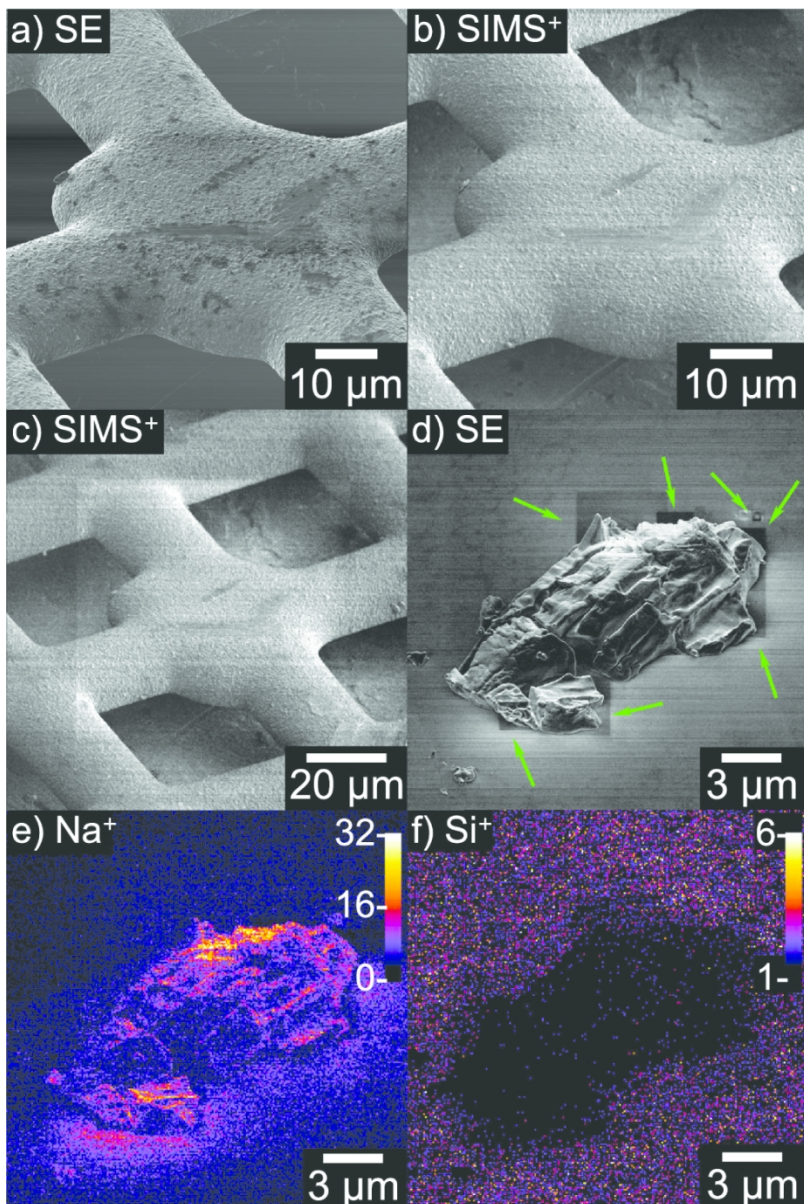


Figure 3. Images of a TEM grid (A-C) and NaCl salt (D-F) crystal generated from the SIMS helium microscope. The SIMS (B,C,E,&F) images are close to the resolution of the microscopy (A&D), demonstrating the power of this technique. This figure is adapted with per-mission from ref145, Klingner, N. et al. Ultramicroscopy 198, 10-17 (2019). Copyright 2019 Science Direct.

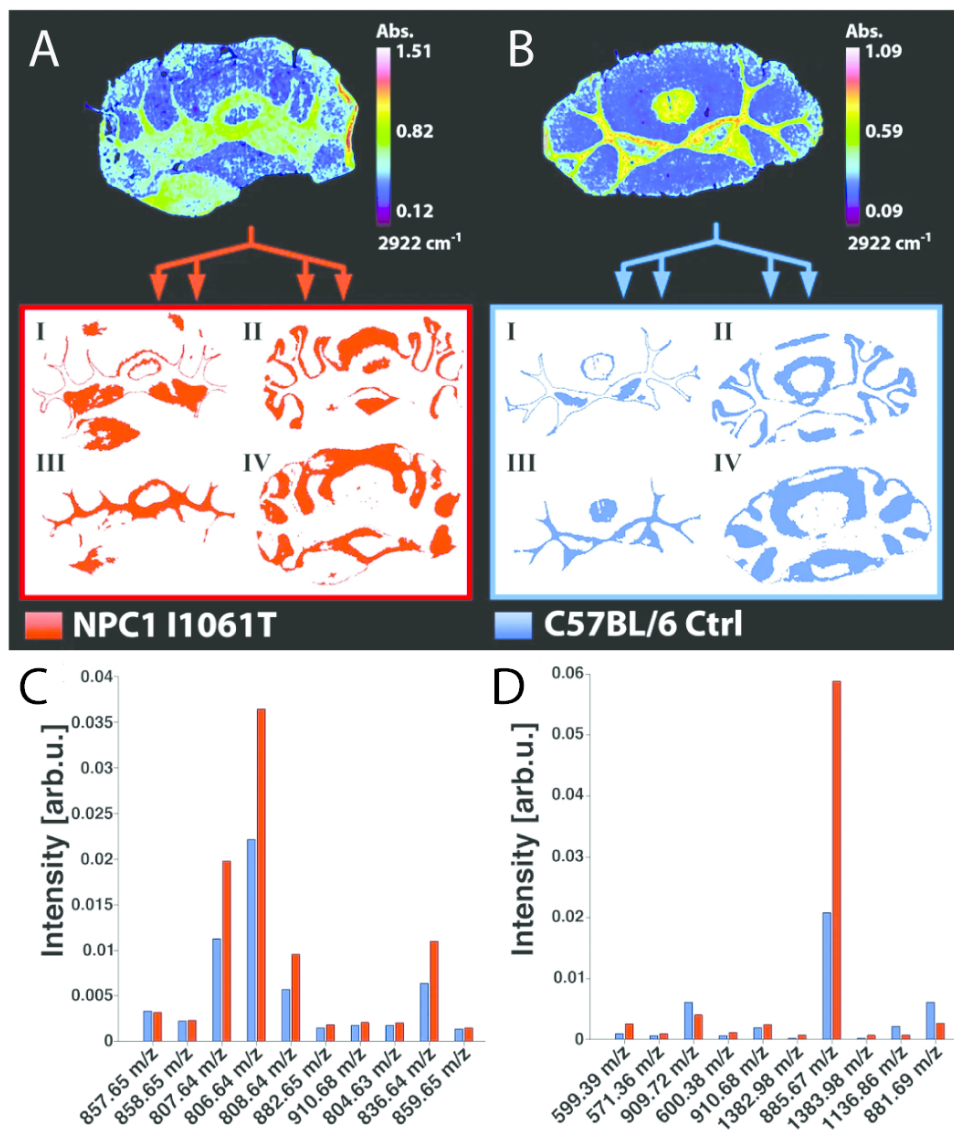
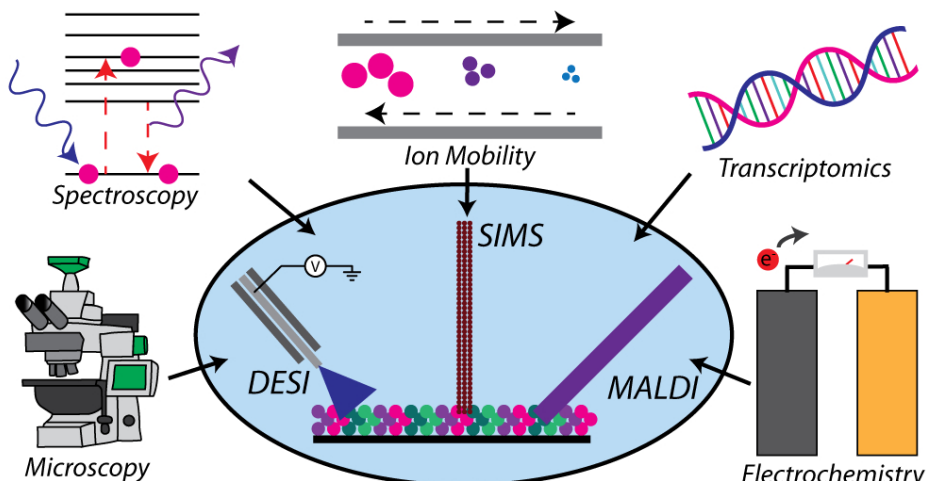


Figure 4. MALDI IMS lipid profiles obtained after FT-IR generated seg-mentation. Murine brain is differentially segmented based on absorbance of 2922 cm^{-1} based on disease (A) and control mice (B). Using this segmen-ta-tion, lipid profiles can be generated for different masks for chemical dif-ferentiation (C-D). This figure is adapted with permission from ref182, Rabe, J. A. et al. Scientific Reports 8, 313 (2018).

Copyright 2018 Nature Publishing.



TOC Graphic